integrity Research Journals

Global Journal of Earth and Environmental Science
Volume 10(4), pages 140-161, August 2025
Article Number: B1273E732
ISSN: 2636-6002
https://doi.org/10.31248/GJEES2024.206
https://integrityresjournals.org/journal/GJEES

Full Length Research

Integrating chemostratigraphy in the modification and improvement of well correlation in the offshore Niger Delta

Ihunda, C. E.*, Selegha Abrakasa and Soronnadi-Ononiwu, G. C.

Department of Geology, University of Port Harcourt, Choba, Port Harcourt, River State, Nigeria.

*Corresponding author. Email: ihundaeze@gmail.com

Received 8th July 2025; Accepted 15th August 2025

ABSTRACT: The Niger Delta is a stratigraphically complex fluvial system of Tertiary age. A total of 15 ditch cutting samples were obtained within the interval of interest, from which 3 wells were subjected to inorganic geochemical and mineralogical analysis to determine the major and trace element concentrations. Inferences from the results show that the Agbada Formation is divided into four Chemostratigraphic mega zones, 12 geochemical units and 9 sand units with geochemical boundaries for DS well at depths of 12,300 ft to 13,500 ft and 7,840 ft to 8,660 ft for ML 1 Well, and ML 2 well at depth 13,240 ft to 14,530 ft. Changes in values of Ga/Rb and Al_2O_3/(CaO+ MgO+K_2O+Na_2O) indicate warmer paleoclimate and increasingly intense hydrolytic weathering, marking a sustained change in the paleoclimate. The high percentage concentration of Al_2O_3 is an indication of abundant clay minerals, whereas the high concentration of Zr suggests sedimentary reworking of the sediments. High V/Ni against Co/Mo ratio concentration intensified upwelling, particularly in those restricted depths was favoured by palaeogeography and significant fluvial input. Conditions could readily evolve from poorly oxygenated to anoxic, the latter state being geochemically the most significant condition. The major oxides trace elements revealed four chemostratigraphic boundaries for DS. ML 1 and ML 2 wells, respectively. The information from V/Sc, Ni/V and V/(V+Ni) ratios indicates the prevalence of anoxic conditions. The redox-sensitive trace elements of the shaly middle parts of the well suggest dysoxic–anoxic conditions, and in most parts of the ML 2 well. Ratios of SiO_2 and Al_2O_3 correspond to sedimentary facies, namely sandstone, siltstone and claystone, while variation in ratios of Cd/Ba and Al_2O_3/(Na_2O+CaO+K_2O+MgO) depicts fluctuating paleoclimate during the deposition of the sedimentary sequence. Geochemical values of Cr/Al_2O_3, Cr/Na_2O and Nb/Al_2O_3 relate to changes in sediment provenance and indicate that during deposition, the provenance became more mafic and less intermediate. The chemostratigraphic correlation is more detailed than is available from other stratigraphic techniques.

Keywords: Chemostratigraphy, trace elements, Miocene, Geochemistry, palaeogeography.

INTRODUCTION

The Tertiary Period is characterised by mixed siliciclastic and carbonate constituents in the stratigraphic profile of the mid–continent (Lane and De Keyser, 1980), which yields complex reservoir lithologies and distributions that are laterally discontinuous and difficult to predict. These complexities have led to nomenclature inconsistencies that complicate correlation efforts and often cause the system to be defined lithostratigraphically and biostratigraphically, and invariably chemostratigraphically (Mazzullo *et al*, 2013; Childress and Grammer, 2015).

In recent decades, the characterization and fingerprinting of individual sedimentary units based on elemental (major and trace elements) and isotopic geochemistry have emerged to be a potential tool for correlation of widely separated strata where there is paucity of biostratigraphic information; this concept is referred to as chemostratigraphy (Ramkumar *et al.,* 2021; Turner *et al.,* 2016). The method is centred on the principle

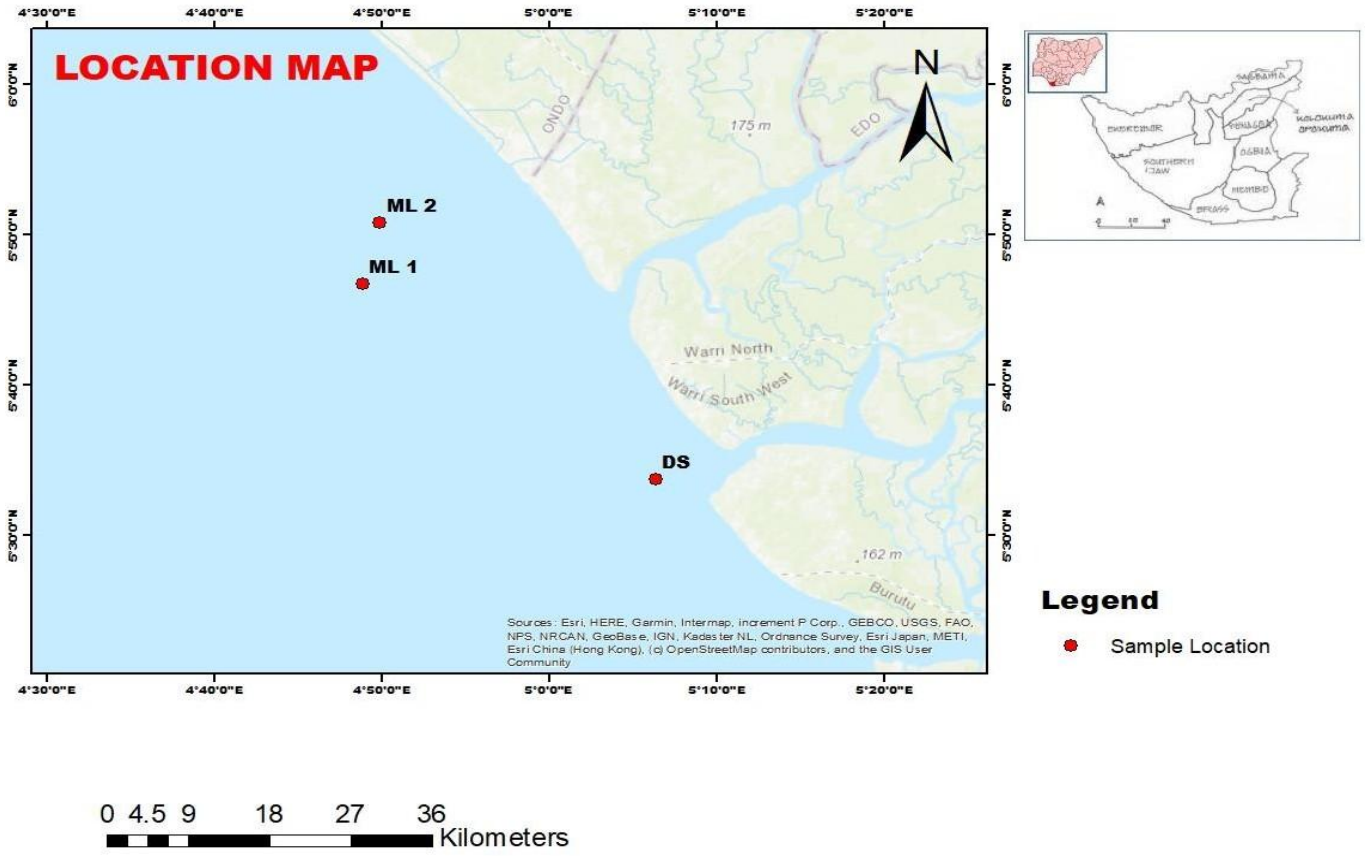

Figure 1. Showing location map of the study Area.

that the chemical composition of sediments is a genuine recorder of the depositional conditions of the sediments and reflects the changes in the paleoredox conditions.

Akaegbobi and Ogungbesan (2016) investigated the depositional environment of the basin using major oxides, trace and rare earth elements. The investigation concluded that restricted to open shallow marine environments, under fluctuating oxidising to anoxic conditions prevailed in the basin, but the study was restricted to the Palaeocene limestones of the basin. Ehinola *et al*. (2016) likewise deduced a probable anoxic condition in quiet, low-energy environments and a rapid rate of sulphate reduction for the Palaeocene limestones. Chemostratigraphy is a trending aspect of Geochemistry which became more frequent in the 1980s, with the oldest publication in 1986 (Ramkumar, 2015). It deals with the fact that sediments are the custodian of records of changes in physical, chemical, biological conditions and events which take place before, during and after their depositions to express paleoclimatic variations, tectonic settings, provenance, reservoir characteristics, paleoenvironments; relating to their source and mechanism associated with their origin in stratigraphic context (Ramkumar, 2015). The present study deals with boreholes that cut across the different lithologic units in the Late Miocene to middle Miocene wells to delineate the geologic history in selected fields in Niger Delta, to infer the variations levels downhole the wells, determine the profile of the trace metal ratio of interest down dip the well of study and to assess the validity and limits of geochemical profiling as a correlation tool in fluvial successions.

Location of study

The study area is located in three depobelts in the Niger Delta offshore. The depobelts with geographic co-ordinates of latitudes 5°33' 42.533" N and 5°6'21.334" E longitude for DS, while ML 1 lies between latitudes 5°46'42'N to 4°48'50" E longitude and ML 2 falls within latitudes 5°50' 48" N and longitude 4°49' 52" E as shown in Figure 1.

Geology and stratigraphy

The stratigraphic sequence of the Niger Delta consists of

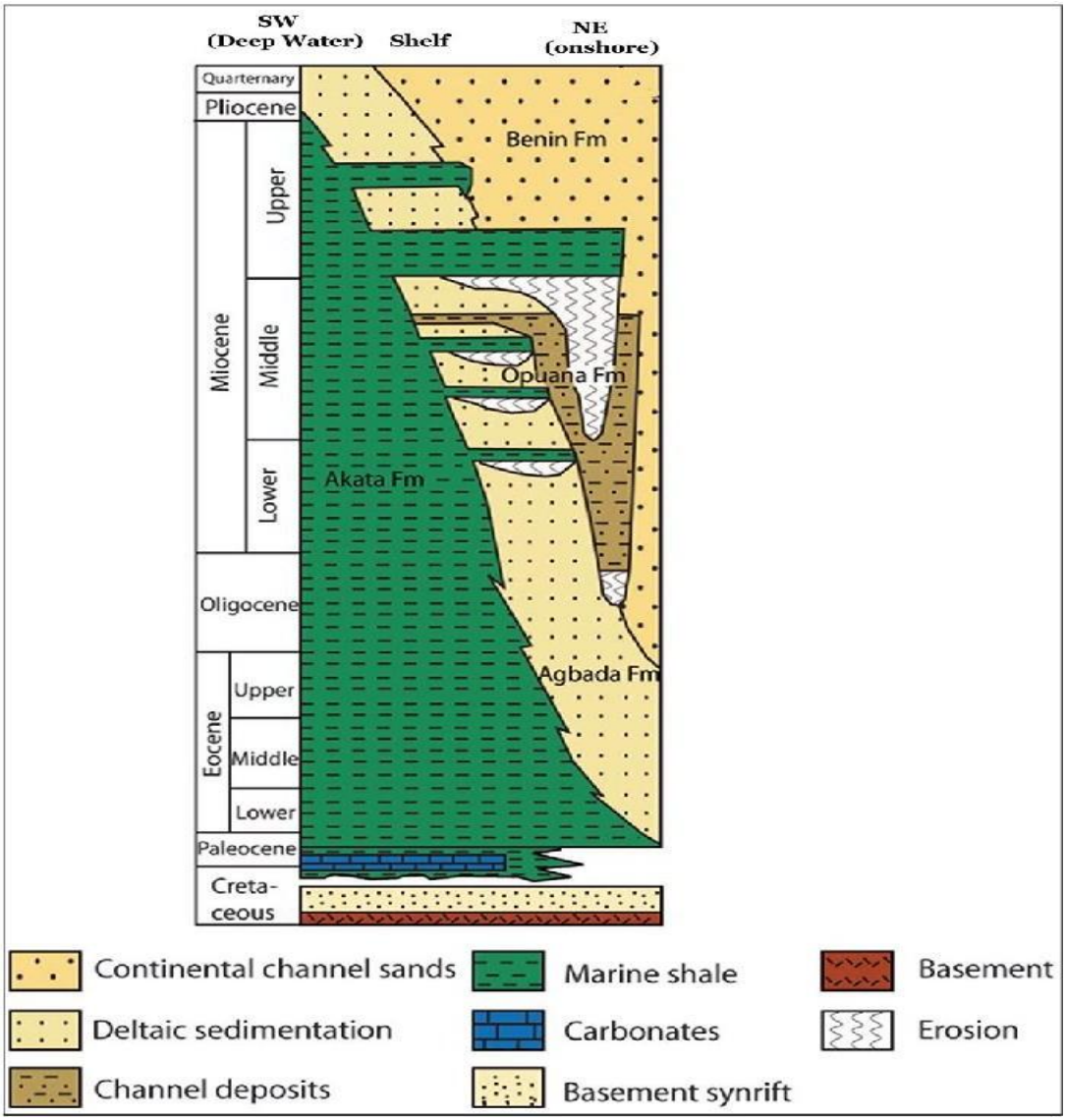

Figure 2. The regional stratigraphic column of the Niger delta Basin shows the three major units in the delta (Akata, Agbada, and Benin formations) (Doust and Omatsola 1990).

coarsening upward sediments that are diachronous (Weber *et al*., 1975; Evamy *et al*., 1978). The Cenozoic Niger Delta Stratigraphy is a direct product of the various depositional environments. The earliest information on the geology of the Niger Delta was reported by Frankl *et al*. (1967), Short and Stauble (1967), and Avbovbo *et al*. (1978) and also in subsequent studies by Evamy *et al*. (1978), Ejedawe *et al*. (1984), Haack *et al*. (2000) and Reijers (2011). Stratigraphically, the delta is divided into three formations, which are the Akata, Agbada and Benin formations (Reijers, 2011). The age of these formations decreases basin-ward, reflecting the general regression of depositional environments within the Niger Delta clastic sedimentary wedge (Figure 2).

MATERIALS AND METHODS

Three boreholes, BH wells namely DS, ML 1and ML 2 wells, were utilised for this study. The samples studied were carefully selected to fall within the age range of the study. The age of the sediments was confined using marker species of palynomorphs and nannofossils. The wells of study fall within the stratigraphic column of interest, as this depth contains a typical Miocene assemblage of palynomorphs of *Gemmamonoporites sp., Psilatricolporites crassus, Verrucatosporites usmensis and Constructipollenites ineffectus*. The presence of Miocene nannofossil marker species of Neochiatozygus modestus. DS, ML 1and ML 2 wells were used to confine

the depth of study. Varied geochemical analysis of major and trace elements was carried out on a total of 15 samples at the National Geosciences Research Laboratories at Barnawa, Kaduna. 15 of the samples are from the study well (sample numbers are depths in ft), The multi-acid, Ultra-trace inductively coupled plasma mass spectrometry ICP-MS (MA250) and whole rock Lithium Fusion ICP finish (LF300) methods were used. The MA250 method is capable of dissolving most minerals, which gives near-total values for about 36 elements. The method was conducted on 15 samples. A 0.25 g split is heated in HNO_3, $HClO_4$ and HF to fuming and taken to dryness, the residue is then dissolved in HCl. The LF300 (ICP/ICP -MS) analysis employs the fusion technique to completely decompose even the most refractory matrices to measure the concentration of the major oxides and loss on ignition (LOI). This was carried out on all 15 samples. A split was taken to represent the original sample and was subjected to quality (QA/QC) control checks during the progression of the analytical portion. The measured concentrations were compared with the Post Archaean Australian Shale (PAAS) (Taylor and McLennan, 1985) and also the average Upper Continental Crust concentrations (McLennan, 2001).

RESULTS AND DISCUSSION

The result of the analysis is summarily presented in the sections, since it is a large data set. However, the log view profiles are represented in Figure 3. The profile consists of log view throughout the well for V/Ni, Y/Nb, Zr/Cr, Rb/Cs, Cr/Na_2O, Na_2O/Al_2O_3, Ga/Rb, Al_2O_3/Bases and (Fe_2O_3+MgO). The shale volume indicates a sandstone formation between 12,300 to 13,500 ft, then intercalations of shale, sandstone, siltstone and carbonate rocks between 7,840 to 8,660 ft. ML 1 wells are mostly carbonate rocks, and from 13,240 to 14,530 ft of ML 2 wells. The value of Fe_2O_3/SiO_2 is low (between 0-16) throughout the same intervals at the bottom of the wells due to the low presence of organic matter and relative formation of pyrite. However, from the middle to uppermost intervals of the three Wells, the value of the Ti/Zr decreases (5-65), but the value of Fe/S increases (4-45) across the same relative intervals in the three wells (Figure 3). These characteristics are presented in Table 1, which shows the summary of the concentrations of the major oxides from the wells.

Chemostratigraphic data of the study wells

The depiction of various log view diagram of kaolinite against Al_2O_3 below shows a weak linear relationship with K_2O (Figure 3). This means that more Al_2O_3 rich minerals could also have been responsible for the distribution of Al_2O_3 in the DS well. K_2O in the DS well was controlled by more than one mineral. For example, in Tables 1 and 2, microcline, illite/muscovite and jarosite were responsible for the distribution of K_2O in the DS well, but microcline exerted more control than other K_2O containing minerals. The depiction of the log view diagram of microcline against K_2O in (Figure 3) showed a weak uphill linear relationship with Al_2O_3, which meant that there were more K_2O rich minerals that were exerting some control in the distribution of K_2O. DS well, but microcline exerted more control than other K_2O containing minerals. The depiction of various log view diagram of microcline against K_2O (Figure 3). The key element Al_2O_3 is primarily controlled by kaolinite, with values of 4.78%. K_2O is mainly controlled by jarosite with a value of 1.14% and /or illite/muscovite. Na_2O was controlled by Na containing minerals, which may have included plagioclase.

These sedimentary complexes are studied lithologically in the areas where (Zr/P_2O_5) phosphorite and Zircon deposits occur in the tectonic structure (Osokin, 1999). The sedimentation coincidence of these sediments has not been established for a long time (Vishnevskaya and Letnikova, 2013). Studies of rare earth and trace elements in carbonate rocks showed that they were formed over a long period of time in the open shelf environment with little to no influence of terrigenous material from the continent and complete absence of volcanogenous and hydrothermal material (Letnikova and Geletii, 2005). So, there is a chance that these sediments recorded the composition of oceanic waters at the time when they were formed, and there is a possibility to determine their sedimentation interval.

Due to the importance of this case point, samples from the base Tertiary in three drilled wells were analysed in the laboratory. The silty claystones immediately above 12,550 ft showed enrichments in Si, Ca and Zr but depletions in Ti and Al. These variations are distinctive and repeated in all three control wells. In sample 12,300 ft; marks an increase in Al_2O_3 with a little decrease in K_2O sandstone and also an increase abundant in Al_2O_3 within depth 12,700 to 13,100 ft which is equivalent to K_2O at 12,700 ft and this elemental mineral is also presence within these depths (Figure 3); but a massive decrease in K_2O and Al_2O_3 but also an abundant increase in Zr and a gradual decrease in P_2O_5 down dip the hole.

Stability of the study wells

The geochemical boundary is shown in Figure 4. From the plot of K_2O and U (ppm), there was a general increase, followed by a decrease at 12,960 ft, and the values trended downward to 12,300 ft, 12,600 ft, 13,290 ft, and 13,500 ft. Above the geochemical boundary at 12960 ft, the trends of K_2O and U (ppm) decrease were generally high, and there was a general increase in trend from the base, showing that the well will collapse at 12,960 ft and is not

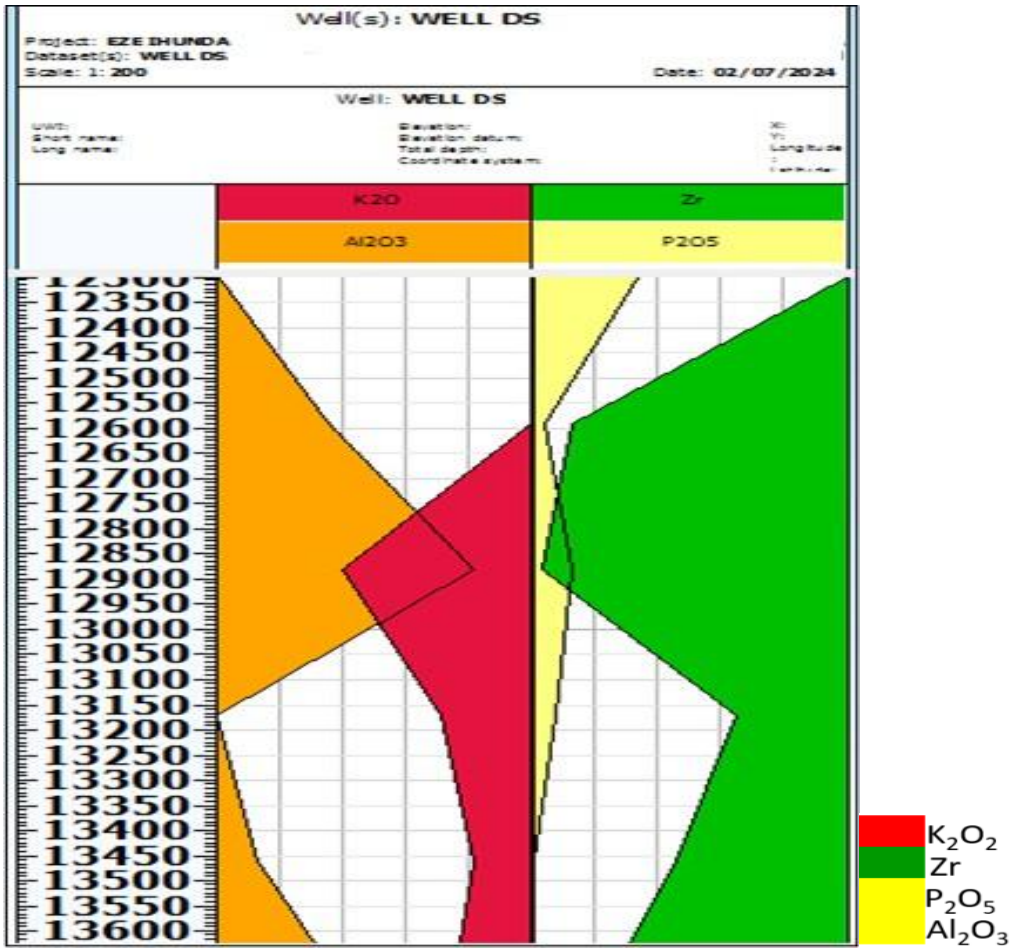

Figure 3. Showing depiction of various log view of DS Well.

Table 1. Major oxides of DS Well for chemostratigraphic characterization.

Depth (ft)	Oxide composition (%)											
	SiO_2	MgO	CaO	K_2O	Na_2O	MnO	P_2O_5	Fe_2O_3	TiO_2	Al_2O_3	SO_3	H_2O
12300	5.06	ND	ND	ND	ND	0.77	0.68	53.08	ND	8.00	4.01	27.60
12630	51.80	ND	ND	ND	ND	0.18	ND	0.38	5.18	12.00	3.16	21.30
12960	48.54	ND	0.02	1.20	0.60	0.36	0.34	6.10	2.74	17.51	ND	22.60
13290	4.20	ND	ND	ND	ND	0.95	0.05	67.90	ND	2.48	ND	24.50
13500	49.13	ND	ND	0.46	0.12	0.18	ND	6.12	4.76	12.48	3.76	22.80

environmentally suitable (Figure 4).

The plot had higher KO_2 values (1.05 to 2.40%) and lower U (ppm) values (0.09 to 0.60%). The averages of KO_2 and U (ppm) values were 2.122 and 0.152%, respectively. It shows that at depth of 12,960 ft, the DS Well has more potassium and hence potentially more susceptible to weathering/erosion and could easily result to well failure due to casing collapse, which is the plot of U (ppm) versus KO_2 for DS well, it indicates that at depth at a 12,960 ft, KO_2 have higher content in the corresponding sediment sample, which is approximately similar to U (ppm) content relative to other samples in the plot (Figure 4). This translates to the greater sediment instability and higher potential for well collapse at 12,960 ft. This should imply that the sandstone formation at depths 12,630 to 13,500 ft bears poor sweep/production efficiency. Given cognisance of the spatial distribution of the studied stratigraphic sections, the phosphorus anomalies could be

Table 2. Trace/minor elements of DS Well for chemostratigraphic characterization.

Elements	12300 ppm	12630 ppm	12960 ppm	13290 ppm	13500 ppm
V	9840.00	5600.00	8400.00	9740.00	4200.00
Cr	380.00	1800.00	2200.00	240.00	700.00
Ca	620,00	800.00	1300.00	3000.00	400.00
Sr	460.00	288.00	401.00	3600.00	211.00
Zr	<0.001	9890.00	9610.00	310.00	8010.00
Ba	201.00	400.00	400.00	220.00	314.00
Zn	B0.00	500.00	512.00	<0.001	500.00
Ce	<0.001	<0.001	<0.001	<0.001	<0.001
Pb	0.780	<0.001	<0.001	<0.001	<0.001
Bi	<0.001	<0.001	<0.001	<0.001	<0.001
Ga	18.50	18.00	<0.001	<0.001	18.50
As	<0.001	1.160	18.50	<0.001	0.950
Nd	<0. 001	<0.001	<0.001	<0.001	<0.001
Y	<0.001	<0.001	<0.001	<0.001	10.00
Ni	3600.00	<0.001	110.00	4300.00	<0.001
Rh	0.480	3.00	0.008	<0.001	<0.001
Mo	6300.00	3410.00	5600.00	5700.00	1200.00
Ti	<0.001	<0.001	<0.001	<0.001	<0.001
Cd	0.060	<0.001	<0.001	<0.001	<0.001
Ru	<0.001	1.410	<0.001	<0.001	1.530
Eu	0.120	<0.001	<0.001	<0.001	<0.001
Re	<0.001	<0.001	<0.001	<0.001	<0.001
Nb	3400.00	<0.001	0.280	3400.00	<0.001
Ta	500.00	<0.001	1.001	461..00	<0.001
W	I 12.00	<0.001	24.00	32.00	<0.001
Hf	<0.001	23.50	51.00	<0.001	26.00
Yb	<0.001	<0.001	<0.001	<0.001	<0.001
Se	<0.00 1	<0.00 1	<0.00 1	<0.00 1	<0.00 1
U	<0.001	<0.001	<0.001	<0.001	<0.001
Th	<0.001	<0.001	<0.001	<0.001	<0.001
Sb	<0.001	<0.001	<0.001	<0.001	<0.001
Ge	21.50	<0.001	12.05	<0.001	6.50
Sn	168.00	38.00	34.00	9840.00	0.084
Pd	<0.001	0.84	<0.001	<0.001	0.770
La	0.118	<0.001	<0.001	<0.001	0.030
Co	<0.001	0.140	<0.001	<0.001	0.170

inferred to have been caused by processes that acted on a regional/basinal scale. P_2O_5 forms an essential ingredient for primary production in the life cycle (Tappan, 1967; Munnecke *et al*., 2010) and is directly connected with oceanic productivity at a global scale (Figure 3). It is interesting to note that the periods of enhanced P_2O_5 accumulation are coincidental with periods of significant reduction of chemical weathering in the source area as indicated by the corresponding negative anomalies which normally result during periods of sea-level rise/high (Rangel *et al*., 2000) and very high K_2O/Al_2O_3 ratio of the rocks when compared negate the possibility of relating these positive anomalies with sea-level maximum and enhanced primary productivity.

Chemostratigraphic zonation characterisation of the DS well

Mega-Zonation 1 (MZ 1)

The MZ 1 runs from 12,300 to 12,600 ft; this mega-zonation dates from the late Miocene. In this sequence, Vanadium contents are relatively lower than Nickel contents, ranging

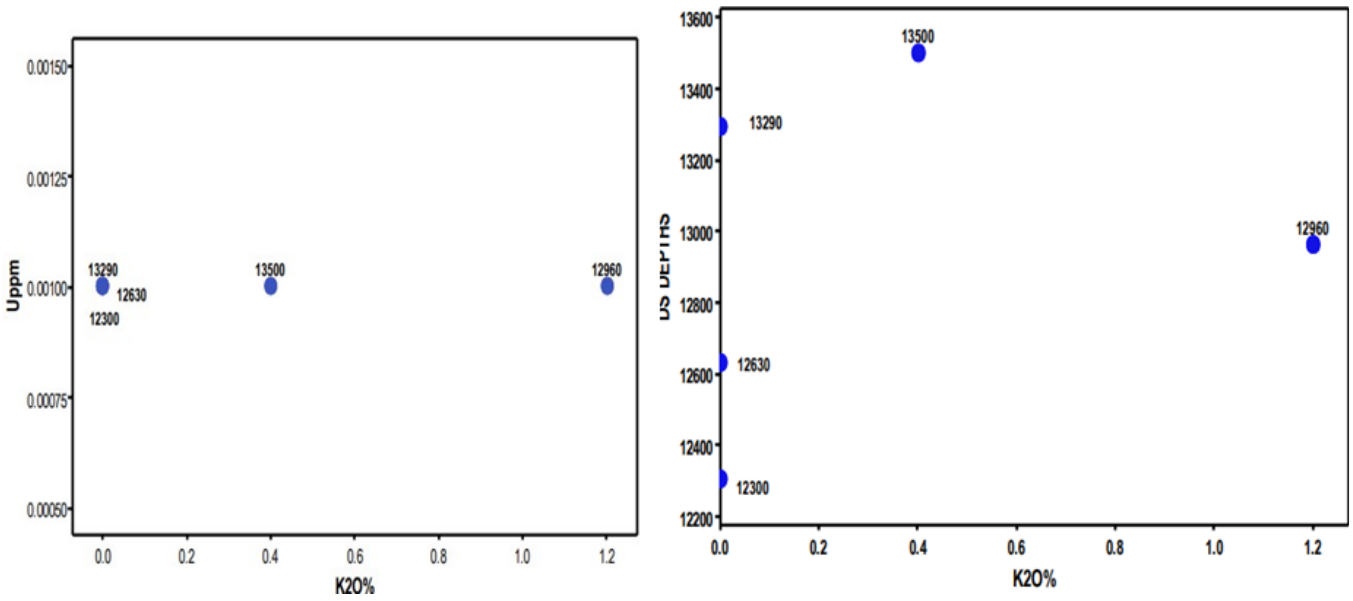

Figure 4. Showing well stability for DS Well of the study area.

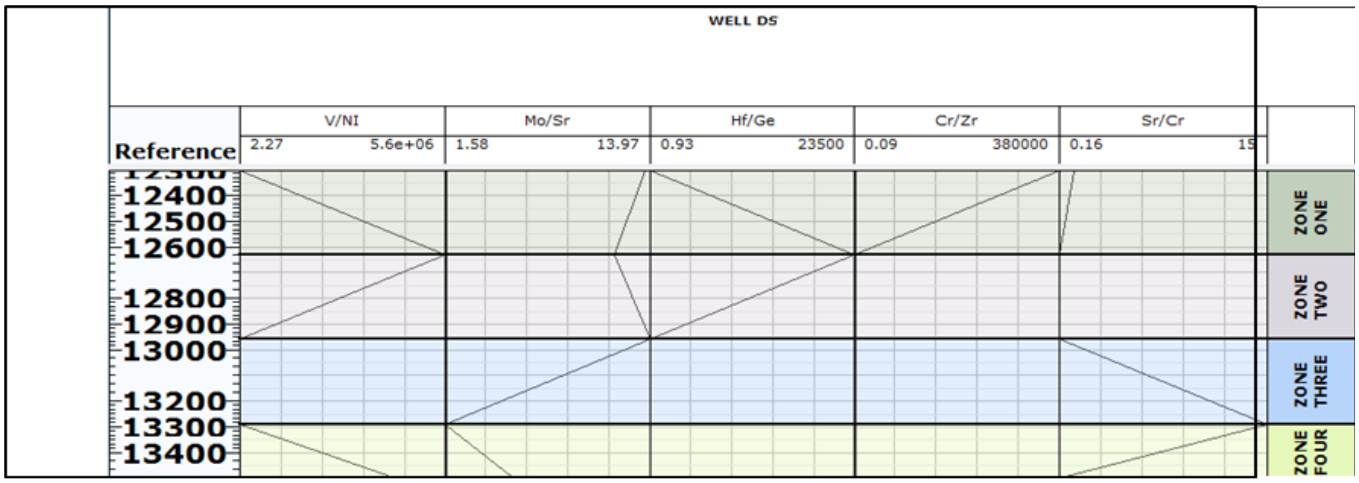

Figure 5. Showing the zonation of DS Well base on elemental ratios.

from 2.7 to 5.6, with an average of 0.6 and a maximum of 0.16; this is the V/Ni ratio. The V/Ni ratio which had been used as indicator of redox environment shows a significant variation, clearly the sandstones intervals such as 12,350 to 12,600 ft and 12,950 to 13,500 ft show very high values which indicates that the sediments were deposited in shallow marginal marine or coastal near shore environment, while depths that have significantly high V/Ni ratios were deposited in marine environment (Figure 5). The depth range of 2,125 to 2,350 ft bears very high V/Ni ratios, which seemingly corresponds to the middle to late Miocene, which has been indicated as the best source rocks (Ramkumar, 2015).

Mega-Zonation 2 (MZ 2)

MZ 2 runs from 12,630 to 12,960 ft. This mega-sequence lies between the Miocene. Mo contents are relatively much lower than Sr contents, ranging from 1.58 to 13.97, with an average Mo/Sr ratio of 0.06. Sr becomes less abundant than Mo. The Mo/Sr ratio markedly discriminates the sandstone rich interval from the shale rich interval, the depth range of 12,600 ft to 12,960 ft indicates high values of Mo/Sr ratio, but with an increase in Hf/Ge ratio shows a corresponds to the interval, which was characterized by widespread deposition of sandstones which could have been sourced from continental clastic rocks.

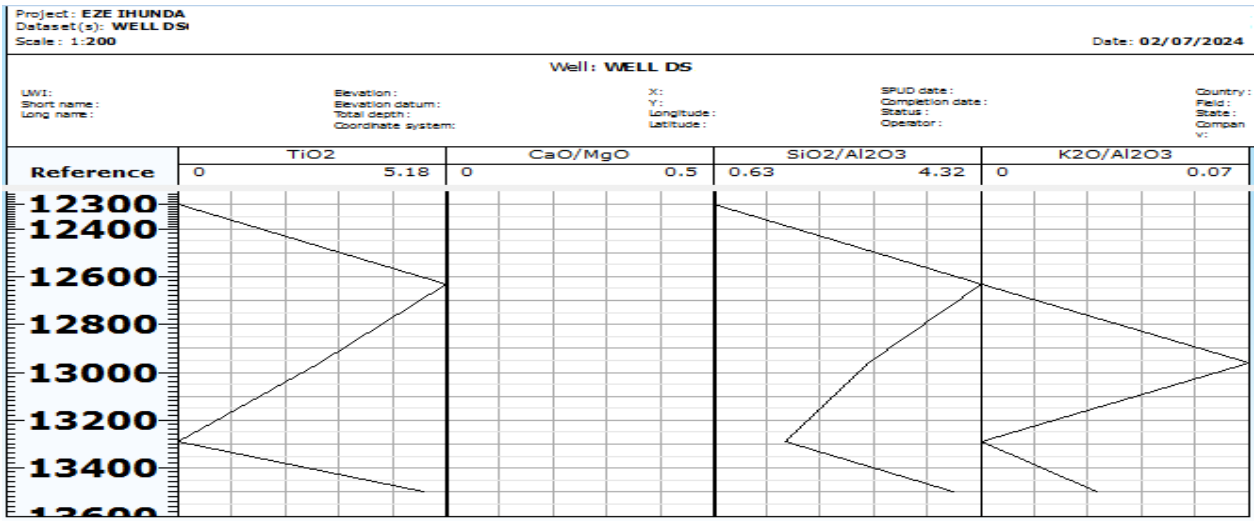

Figure 6. Showing the zonation of DS Well base on major oxides ratios.

Mega-Zonation 3 (MZ 3)

The MZ 3 starts from 12,960 to 13,300 ft; this mega-sequence dates from the late Miocene. In this zone, V/Ni ratio grades are relatively higher than Mo/Sr grades, ranging from 1.58 to 13.97, with an average of 0.5 for the Hf/Ge ratio. Cr/Zr ratio is 0.5, which follows the Sr/Cr trend, with contents ranging from 0.16 to 15 for Cr/Zr and a ratio of for Hf/Ge (Figure 6). These grades are the same in both DS and ML 2 wells, and the behaviour of the sediments in both wells is the same. This will enable us to make a correlation between these wells.

Mega-Zonation 4 (MZ 4)

MZ 4 starts from 13,300 to 13,500 ft. This mega-sequence lies between the Early-Late Miocene. V/Ni contents are relatively higher than Mo/Sr contents, ranging from 1.58 to 13.97, with an average Mo/Sr ratio of 0.06, which is also lower than Sr/Cr ratios. The absence of Hf/Ge and Cr/Zr ratios is very significant; as a result, concentrations of these elements are influenced mainly by the abundance and distribution of illite, smectite and mica, to a lesser degree (Figure 6). In any siliciclastic sequence, the primary differences in whole rock geochemistry occur between lithologies (Ratcliffe *et al*., 2007). The SiO_2 and Al_2O_3 have been used to understand the relationship between sandstone and clay in sediments. In this study (Figure 6), a binary plot of SiO_2 and Al_2O_3 shows a linear relationship for both SiO_2 and Al_2O_3, with a ratio of 0.6-4.3 for all the samples from the wellbore. However, the majority of the samples occur between 30 to 60% of silica relatively with high value ratio of 14-27 in Al_2O_3/K_2O, compared to a low value ratio of 0.2-0.5 K_2O/Al_2O at depth 13,290 to 13,500 ft.

Change in paleosalinity

Salinity affects the water stratification in a lacustrine or marine basin and has a marked influence on the development of source rocks. The paleowater salinity is usually determined according to the differential accumulation of elements. Ba can precipitate after combining with other elements. Ba is less soluble, while Ba^{2+} is prone to combine with SO_4^{2-} to generate $BaSO_4$, which will precipitate (Sun *et al*., 2013; Song *et al*., 2017; Li *et al*., 2019a; Zhang *et al*., 2020). Ba will precipitate at the bottom of a water body when the salinity rises to a certain level, Sr can migrate more easily than Ba, and Sr will precipitate only when the salinity is very high (Xi *et al*., 2011; Fu *et al*., 2016; Wang *et al*., 2018; Zhang *et al*., 2020). Thus, the presence of Sr in the samples is thought to have originated from the clay fraction instead of carbonate-hosted Sr, except for a few samples with high CaO content. The Sr/Ba value is 0.91–16.35 (average of 3.45) for the DS well samples, and 1.09–2.68 (average 0.75) for the ML 1 well samples, indicating that the DS well formation was deposited in a fresh water environment (salt water environment occasionally) (especially for DS well at depth 13,290 ft). Rb/K is also an effective index for determining the salinity of paleowater (Zhang *et al*., 2020; Zhang X. *et al*., 2021). For the DS well samples and 0.7–0.45 (average 0.43) for the ML 1 well samples, suggesting that the Middle – Late Miocene were deposited in a fresh–brackish water environment with an upward increase in salinity. The Sr/Ba and Rb*1000/K values increase from the bottom to the top in DS well at depth 12,300 ft and ML 2 well at depth 14,530 ft, indicating that the Middle – Late Miocene were deposited in a fresh–brackish water environment with an upward increase in salinity which may suggest the increased inflow of seawater into the marine

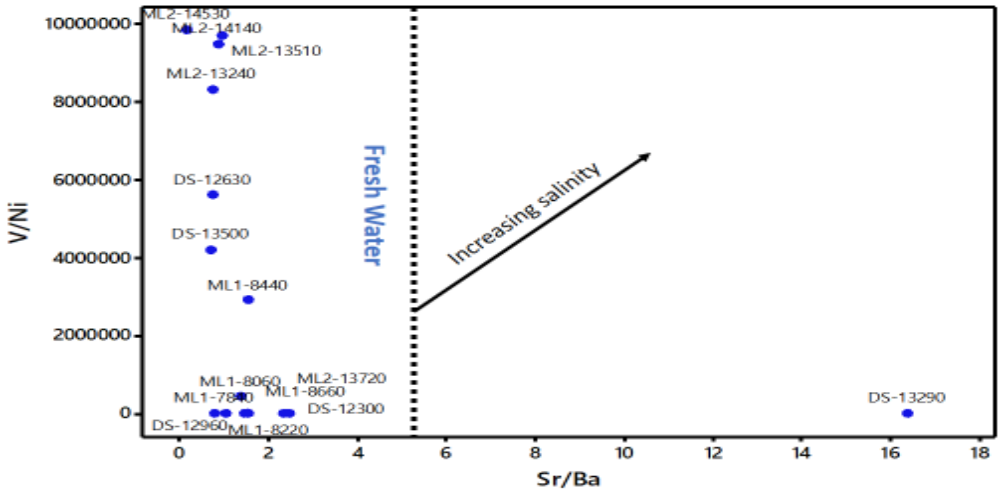

Figure 7. Showing Sr/Ba *versus* V/Ni showing the depositional environment (adopted after Jia *et al*., 2013).

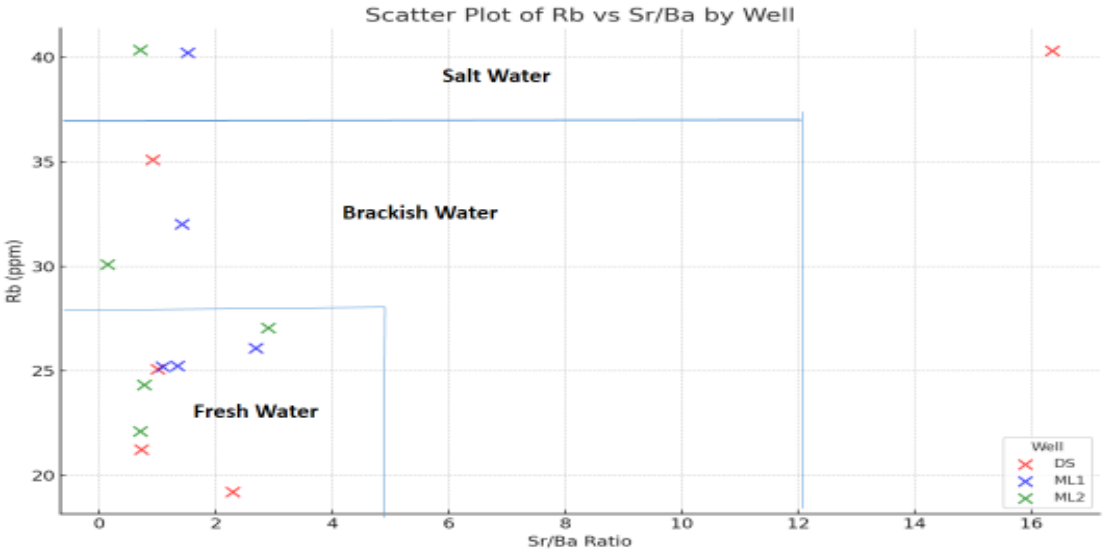

Figure 8. Paleosanilty scatter plots of Sr/Ba and Rb indicating depositional environment of the study wells.

sedimentary rocks have higher B and lower Ga contents than those derived from fresh water environments (Figure 8).

Therefore, for the ML 1 well samples indicating a continental fresh water environment. It is thus inferred that the Middle–Late Miocene ages in the ML 2 well were deposited in a fresh–brackish water environment, with the paleosalinity increasing from the DS well to the ML 2 well (Figure 7). This finding is also supported by the paly-ecological community in this interval comprises moderately low occurrences of marine, savanna and coastal elements and moderately high occurrences of freshwater indicators.

Change in Terrigenous clastic input

Basically, Al, Zr and Ti are highly resistant accessory elements and less sensitive to weathering or diagenetic processes (Murphy *et al*., 2000; Calvert and Pedersen, 2007; Ross and Bustin, 2009; Wei and Algeo, 2020). They are useful indicators of detrital influx (Zhang *et al*., 2021; Li *et al*., 2021; Song *et al*., 2021; Xin *et al*., 2021). Besides, Th/Al is a key indicator to reveal the intensity of terrigenous clastic input. The Ti, Zr and Al_2O_3 profiles for ML 1 Well show similar patterns, with a relatively stable trend that is associated with the chemical weathering intensity or water depth (Figures 5 and 9). Detrital proxies of the samples

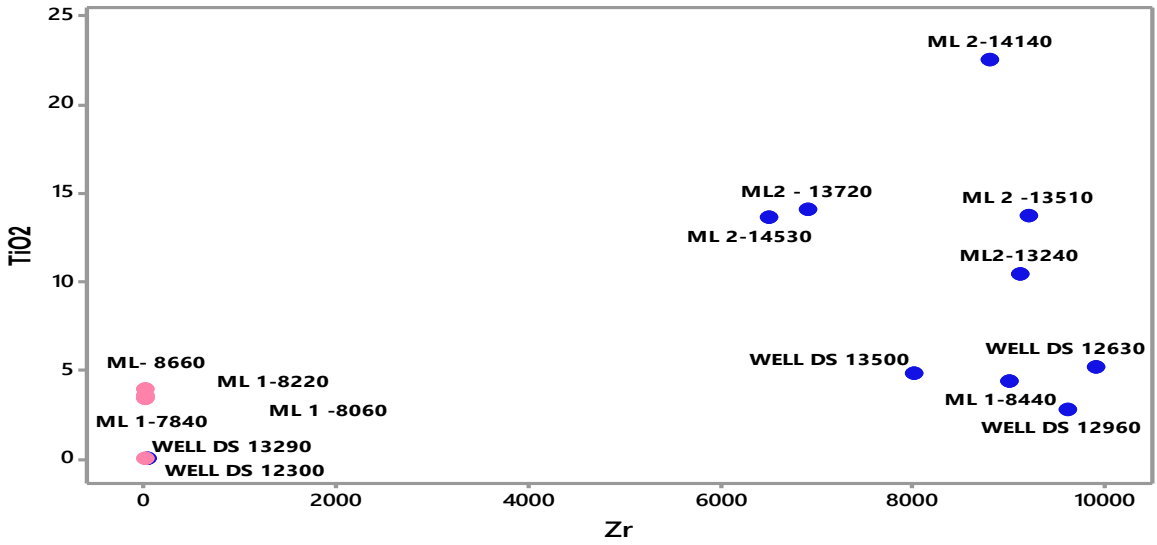

Figure 9. Plot of TiO_2 and Zr for discriminating terrigenous input source rock.

from ML 2 Well suggest that the terrigenous flux varies significantly from the ML1 well to the DS well and increases upward (Figure 9).

Evolution of depositional environment and organic matter enrichment model

V/Ni and Co×Mo are proposed as effective proxies to distinguish upwelling and hydrographic restricted settings (Sweere *et al*., 2016; Wu *et al*., 2022; Zhu *et al*., 2022). Generally, sediments in upwelling systems are characterised by Mn and Co depletion, while sediments in restricted basins show elevated Mo and Co values (Sweere *et al*., 2016). The principle of the Cd/Mo proxy lies in the different behaviours of V and Ni in seawater. V has a close link to primary productivity and displays a nutrient-like profile in the water column, while Mo behaves conservatively (Zhu *et al*., 2022).

Thus, low Co×Mo (<0.4) or low Mo_{EF}×Co_{EF} (<0.5) are typical for coastal upwelling settings, while high Co×Mo (>0.4) and high Co_{EF}×Mo_{EF} (>2) for restricted settings like the Black Sea (Zhu *et al*., 2022). The Co×Mo values of the DS well and ML 1 well samples cover a wide range (1.36–7.00, avg. 0.000126), with the average lower than 0.4 (Figure 10). According to the Co*Mn–V/Ni plot (Figure 10), the samples in this study were formed in open/upwelling water conditions, and their organic matter enrichment was mainly controlled by preservation conditions (Table 3). Climate during the deposition phase can influence the seawater environment (i.e., depth, salinity, stratification, and aquatic biomass), and the evolution of depositional environment controls the input, deposition and preservation of organic matters (Meng *et al*., 2012; Li *et al*., 2016; Shen *et al*., 2017; Li *et al*., 2019b; Li *et al*., 2021; Zhang *et al*., 2020; Xin *et al*., 2021; Hou *et al*., 2022). According to the geochemical analyses, the Miocene strata in the ML 2 well of the study area were deposited in a semi-arid to humid/warm climate and suboxic-anoxic fresh water environment with relatively large detrital input and stable water depth. During the deposition of the DS well and ML 1 well of the study wells, the ML 2 well mainly developed braided river deltas, beach bars and fan deltas (Zeng *et al*., 2019). Apparently, the DS well has a relatively low salinity compared to the ML 1 well, and considerable variations from fresh water to brackish in the ML 1 well (Figure 10). A closed water system existed during the deposition of the DS well, and the sea level rose during the deposition of the ML 2 well, making the seawater flow over the ML 2 well. The open/upwelling basin was more connected with the ocean and evolved into a semi-open/upwelling basin. Brackish water may cause water stratification and produce a strongly anoxic environment with excellent preservation conditions. Therefore, it is believed that both primary productivity and preservation conditions played essential roles in controlling the enrichment of organic matter in the ML 2 well, and the latter resulted from the open/upwelling water setting (Figure 10).

Change in Paleoredox

In the case of certain elements, which are sensitive to redox changes in the marine environment and pore waters, they are used for reconstruction of redox conditions in young and ancient sedimentary basins associated with organic material deposits and sulphide

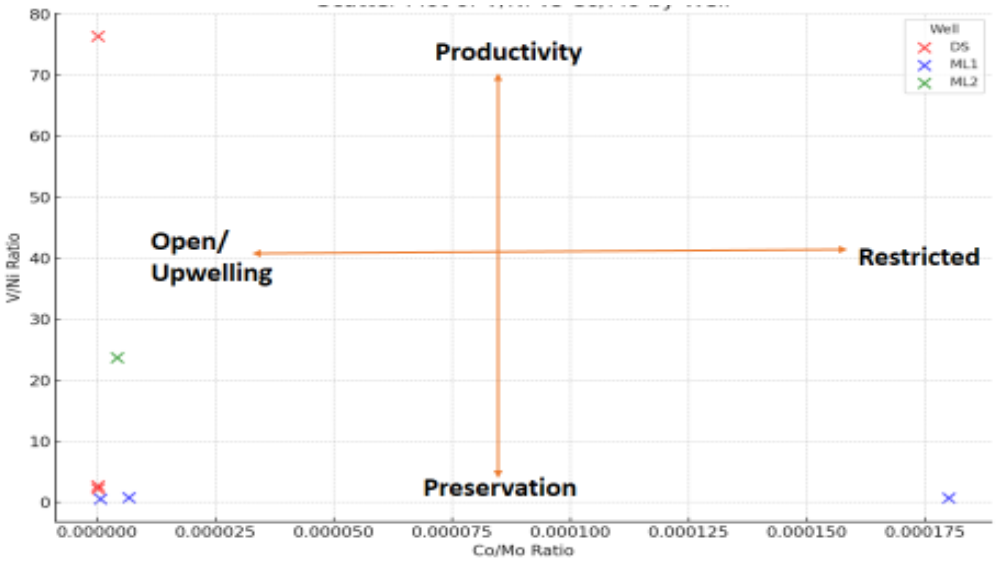

Figure 10. Scatter plot of V/Ni /Co/Mo. The position of the lines is roughly the boundaries amongst various settings (adopted from Sweere *et al*., 2016).

Table 3. Comparative average weight percentage elemental ratios of the study wells.

Well	Depth	V/Ni	Co/Mo	Th/Sr	Zr/Sr	Rb	Sr/Ba
DS	12300	2.7333	1.60E-07	0	0	19.21	2.28856
DS	12630	–	4.11E-05	0	34.34091	21.24	0.72
DS	12960	76.3636	1.80E-07	0	23.9601	25.07	1.0025
DS	13290	2.2651	1.80E-07	0	0.08611	40.31	16.3636
DS	13500	–	1.42E-04	0	27.8125	35.09	0.91624
ML1	7840	0.6133	6.70E-07	0	0	25.2	1.09091
ML1	8060	–	5.00E-05	0	0	25.23	1.34375
ML1	8220	0.765	6.67E-06	0	0	26.08	2.6875
ML1	8440	–	1.36E-03	0	19.2	40.23	1.51515
ML1	8660	0.7017	1.80E-04	0	0	32.02	1.41667
ML2	13240	–	1.14E-04	0	30.13245	22.1	0.70233
ML2	13510	–	1.67E-04	0	25.5556	24.33	0.77436
ML2	13720	23.72	4.17E-06	0	19.1667	27.05	2.90323
ML2	14140	–	7.00E-05	0	29.3548	40.35	0.70588
ML2	14530	–	1.89E-04	0.00645	21.6667	30.08	0.144
Average wt %		15.86	0.000126	0.00645	19.98	28.09	1.54

occurrences in oxygen-deficient media (Brumsack, 2006; Tribovillard *et al*., 2006). Several trace elements, such as Mo, Mn, Ni, V, U, Cr, and Co, have been used to evaluate paleoredox conditions (Hatch and Leventhal, 1992; Jones and Manning, 1994; Algeo and Maynard, 2004; Rimmer *et al*., 2004). Previous studies proposed different criteria for V/(V+Ni), according to Hatch and Leventhal (1992) and Wu *et al*. (2022), a high V/ (V+Ni) value (≥0.84) reflects water column stratification and indicate anoxic bottom water, and this value range from 0.54 to 0.72 reflects a dysoxic environment with weak stratification of the water column, while a low value (0.46–0.60) reflects an oxic environment (Table 4). Selegha *et al.* (2020) concluded that the V/Ni ratio indicates redox environment, the ratio indicates that the sandstone at depths of 12,300 to 14,140 ft and 8,220 ft were deposited in oxygen oxygen-rich nearshore environment or shallow marine environment, which bear very high values indicating more marine environments. Lewan (1984) suggested that the V/Ni ratio in crude oil, which is not altered by diagenesis, reflects

Table 4. Shows elemental ratios and their critical values for particular environment.

Elemental ratios	Oxic	Dysoxic	Anoxic	Euxinic	Source	Present study
Ni/Co	<5	5-7	>7	-	Jones and Manning (1994)	4.3-4000
V/Cr	<2	2-4.5	>4.5	-	Dill *et al*. (1988)	27.67-4000
V/(V+Ni)	<0.46	0.46-0.60	0.54- 0.82	>0.84	Hatch and Laventhal (1992)	0.38-1

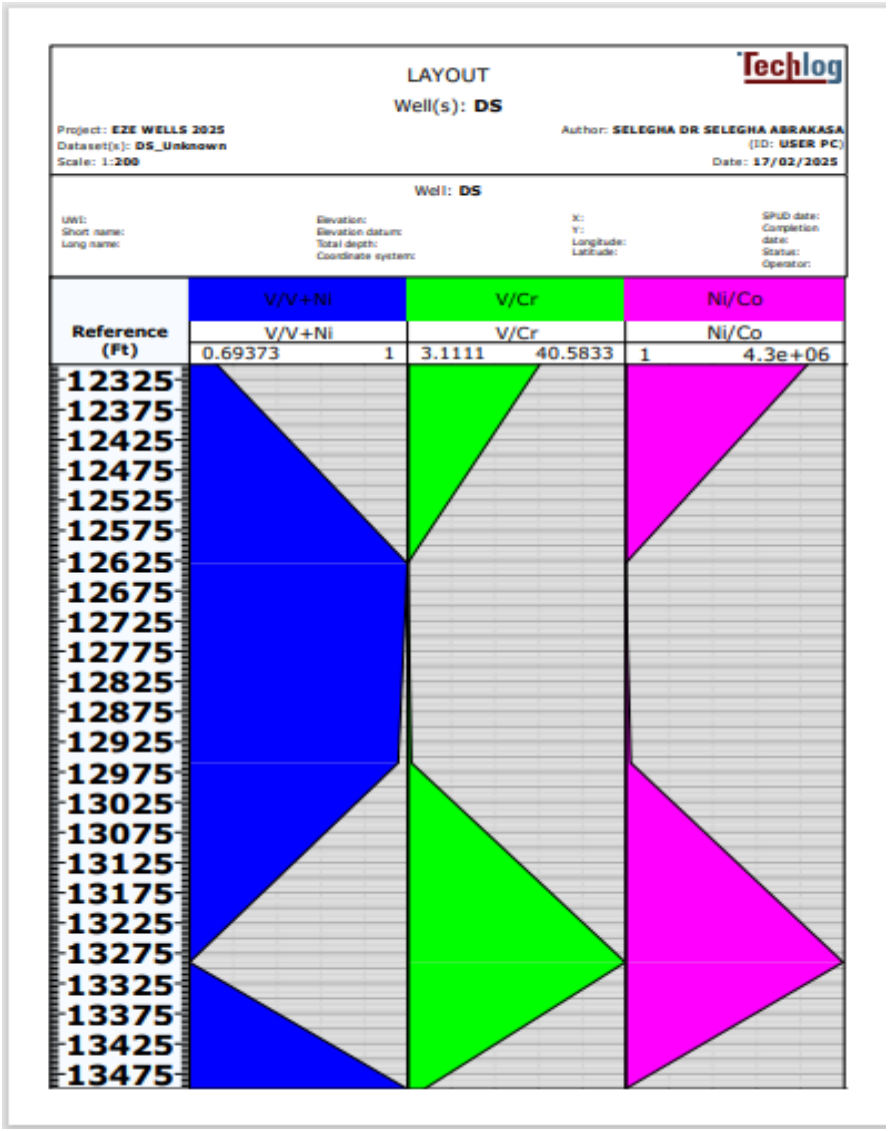

Figure 11. Paleoredox Conditions of the Carbonaceous Shale Cutting of the wells.

environmental conditions during its deposition. He showed that the V/ (V+Ni) ratio for organics forming under euxinic conditions is greater than 0.50. According to Hatch and Leventhal (1992), V/ (V+Ni) ratios are greater than 0.84 for euxinic conditions, in the range of 0.54 – 0.82 for anoxic conditions and between 0.46 and 0.60 for dioxic conditions. Vanadium (V), which is incorporated into tetrapyrrole structure under anoxic conditions, may also be precipitated by adsorbing onto the surface of clay minerals, which most probably occurs after burial (Breit and Wanty, 1991). The V/V+Ni ratios of the DS, ML 1 and ML 2 well indicate anoxic and euxinic conditions during the deposition of the study section of the wells (Figure 11). Chromium (Cr) and cobalt (Co) concentrations enrichment

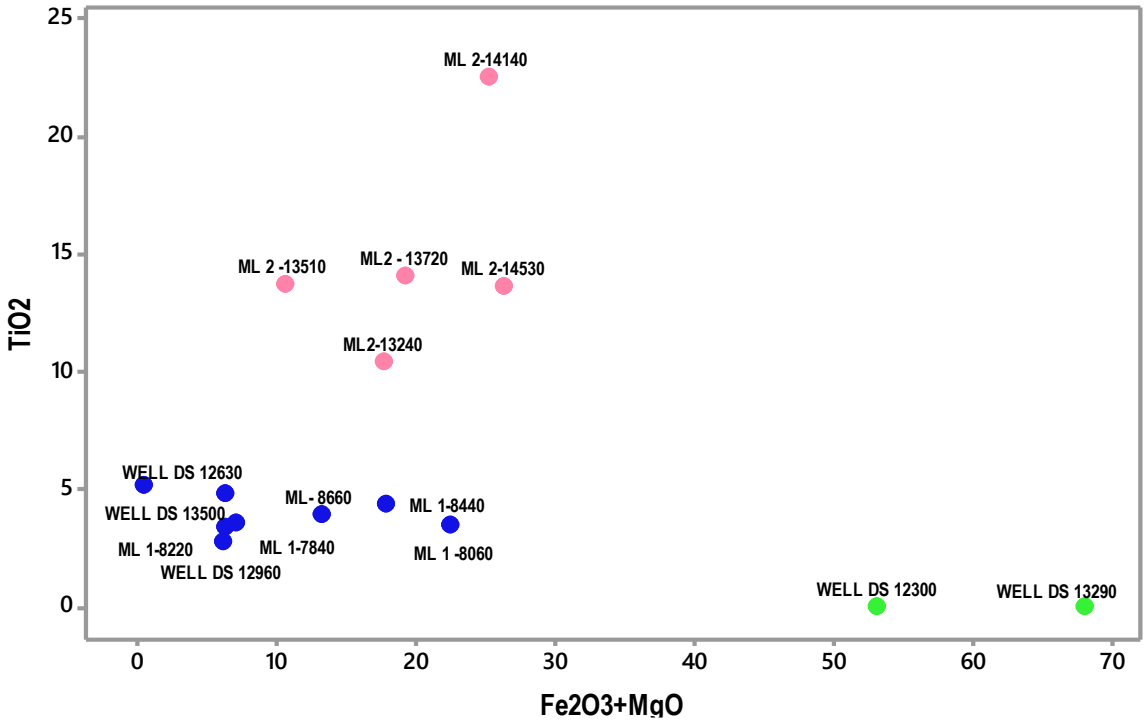

Figure 12. Plot of TiO_2 and (Fe_2O_3+MgO) for delineating tectonic setting for sandstone from the study wells.

in ditch cutting are believed to be of the detrital fraction and not affect by redox conditions (Ross and Bustin, 2006). Both Ni and Co are incorporated into the pyrite structure. High Ni/Co ratios are believed to be related to anoxic conditions (Jones and Manning, 1994). The Ni/Co ratios for the study section of the wells suggest anoxic conditions, tending towards euxinic conditions due to their extremely high values (Figure 11).

Change in plate tectonic setting

The knowledge of the plate tectonic setting of a basin is important for the exploration of petroleum and other resources, as well as for palaeogeography. The major elements geochemistry of the sandstones can be used for drawing inferences related to the provenance type and the plate tectonic setting of ancient sedimentary basins (Armstrong-Altrin *et al*., 2004; Bhatia, 1983; Roser and Korsch, 1986). Siliciclastic rocks from oceanic arc, continental arc, active and passive continental margins have variable composition, especially in their Fe_2O_3 + MgO, Al_2O_3/SiO_2, K_2O/Na_2O, and $Al_2O_3/(CaO + Na_2O)$ ratios (Bhatia, 1983; Sarı and Koca, 2012; Madukwe *et al*., 2015). Three plate tectonic settings: passive continental margin PM, active continental margin ACM, and oceanic island arc (ARC) are recognised on the K_2O/Na_2O versus SiO_2, Al_2O_3/SiO_2 versus K_2O/Na_2O discrimination plots of Roser and Korsch (1986) (Figures 12 and 13). The plots reveal that the sediments of ML 2 well were deposited in a passive tectonic margin setting. They may also be classified as mafic (Magnesium and Iron-rich) or felsic (Feldspar and Silicon-rich); the former consists mostly of oceanic crust, while the latter consists mostly of continental crust. Figure 12 a plot of TiO_2 and (Fe_2O_3+MgO) for the sandstones from of DS, ML 1 and ML2 with depths 12,300-13,500ft; 7,840ft-8,660ft and 13,240ft to 14530ft indicate that the Upper series (B) have high (Fe_2O_3+MgO) and TiO_2, this might suggest introduction of weathering products from Oceanic Crust, however most of the Lower series (A) have low (Fe_2O_3+MgO) and TiO_2 indicating contributions from Continental Crust. This may imply that during the deposition of the upper series (B), there could have been a tectonic event that led to the production of basaltic lava, which later weathered into heavy sandstone, which was deposited as the upper series. Von Rad *et al*. (1982) recorded extrusions from the volcanics around the area within the Cameroon basin; this could be the source of the heavy sands Selegha *et al.* (2020). Figure 13, which is a plot of TiO_2 and (Fe_2O_3+MgO) for the formations transversed by the wellbore, also shows that most of the formation are consisted of high values of TiO_2 and (Fe_2O_3+MgO) which indicated that they were sourced from basaltic rocks from Oceanic Crust (Mohriak *et al*., 2000; Nairn and Stahli, 1974; Nemcok, 2016; V on Rad *et al*.,

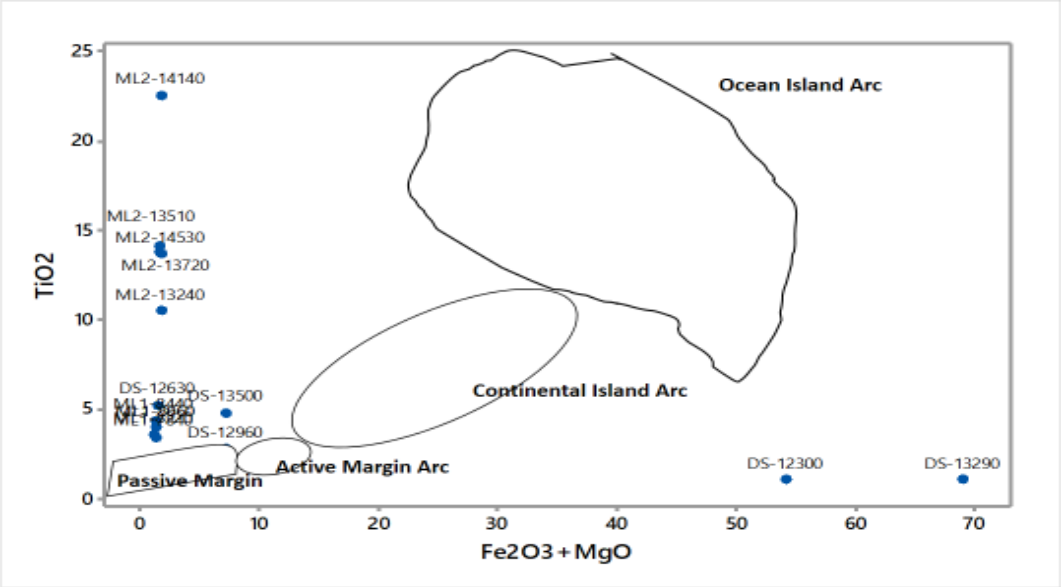

Figure 13. Discriminating tectonic settings diagram by major element compositions.

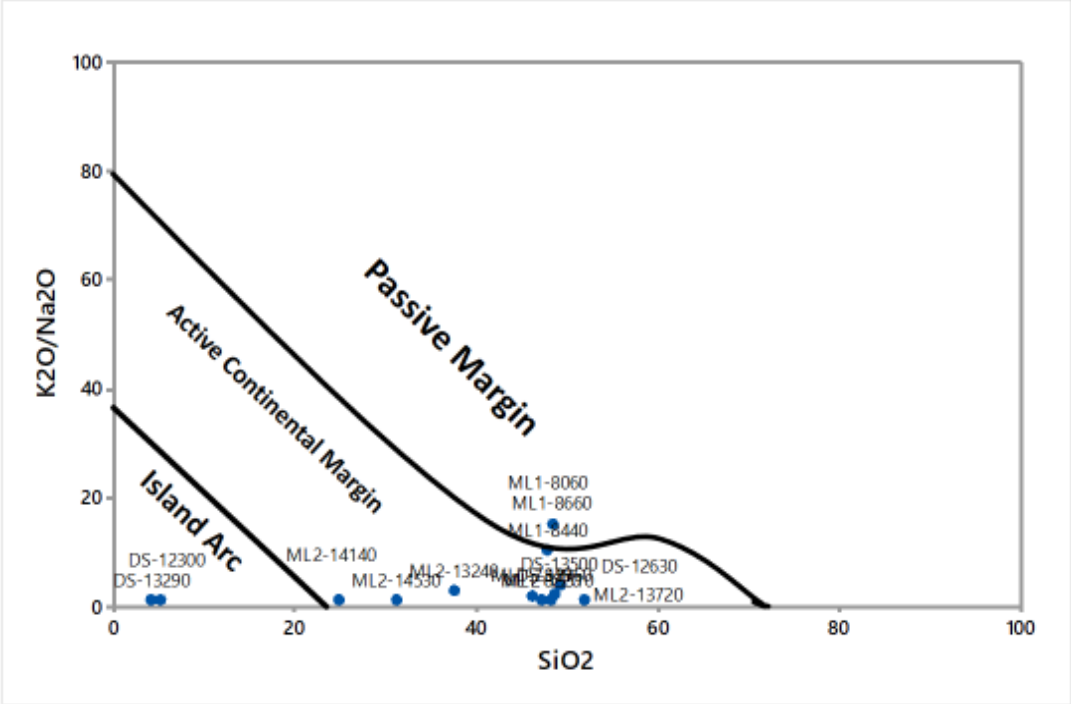

Figure 14. major and trace elemental oxides diagram for tectonic settings.

1982). The tectonic setting for the upper series (B) in Figure 12 is that of the Continental Island, and for the lower series (A) Passive Continental margin. The ratios of K_2O/Na_2O variation with SiO_2 are plotted in a binary diagram (Roser and Korsch, 1986) to understand the tectonic setting of sandstones. It is found that all the samples are plotted in the active continental margin field (Figures 12 to 15). The same pattern is observed when the sandstone samples are plotted on the SiO_2/Al_2O_3 versus $Na_2O + K_2O$ diagram of Roser and Korsch (1986).

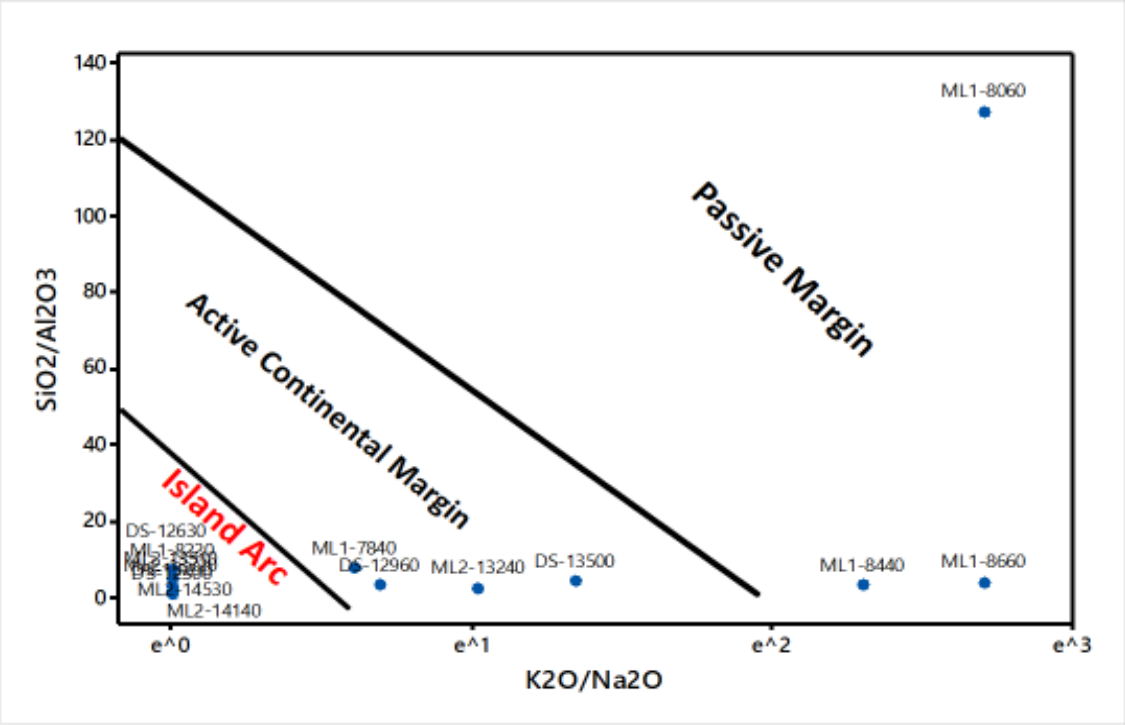

Figure 15. Major and trace elemental oxides diagram for discriminating tectonic settings.

Change in provenance and paleoclimate

Clay minerals in sediments can be useful indicators of paleoclimatic conditions and provenance, particularly when the sedimentary basins are small (Von Eynatten and Gaupp, 1999). According to Churchman (2000), the two-layer/three-layer clay mineral ratio is mainly controlled by climate. Warm and humid conditions are typical for kaolinite formation (Chamley, 1989; Hallam *et al*., 1991; Islam *et al*., 2002; Ghandour *et al*., 2003; Odoma *et al*., 2013). The presence of kaolinite indicates a warm, humid tropical climate for the source area where the sediments were derived. It further indicates that the rocks were deposited in a marginal marine setting due to its hydraulic sorting (Ghandour *et al*., 2003).

Al_2O_3/ K_2O ratio has been used to suggest precipitation (rainfall) rates (Aplin, 1993). If Al_2O_3/ K_2O ratio is less than 1.00, then precipitation (rainfall) is low. Al_2O_3/K_2O ratio higher than 1.00 suggests high precipitation (rainfall). The ratio for the study well varies from 14.59 to 62.53 (Average 39.12) (Table 5). This indicates that the precipitation (rainfall) was high.

The Al_2O_3/TiO_2 ratio serves as a climate indicator for the provenance area (Maslov *et al*., 2003). If Al_2O_3/TiO_2 ratio is less than 20, then the climate is humid, but if it is greater than 30, it is an arid climate (Table 5). The values of the Al_2O_3/TiO_2 ratio from the study wells vary from 0.22 to 6.71 (average 3.40). This suggests that the climate was humid.

Provenance analysis reconstructs the source region, size and setting of the source region, climate and relief in the source region, the specific types of sedimentary rocks and the distance and transport direction travelled by the sediments (Pettijohn *et al*. 1987; Von Eynatten and Gaupp 1999).

In respect of paleoclimate, the Zr/Sr ratio, which represents the kaolinite/illite ratio, may give an insight, correlating it with the Al/bases ratio (Figure 16). In this study, the Zr/Sr ratio has a positive correlation with the Al/bases ratio (Figure 16). This implies that the formation of kaolinite increases with hydrolytic weathering, and kaolinite are formed in hot humid climates, while illites are formed in drier, cooler climates (Craigie, 2018; Ramkumar, 2015). In the context of reservoir pore morphology, the preferential formation of kaolinite should indicate the occurrence of pore-filling minerals in the reservoir sandstones. This should imply that the sandstone formation of the DS well at 12,630 to 12,960 ft and also for ML 1 at depth 8,060 to 8,220 ft to depth 13,510 to 13,720 ft of ML 2 well bear poor sweep/production efficiency. While the thin sandstone formation in the deeper series bears less kaolinite and less pore-filling minerals, corresponding to better production efficiency comparatively. Strong correlation between Chromium (Cr) and Nickel (Ni) and high concentrations of both elements have been used by several authors to determine sources of the sedimentary rocks (Hiscott, 1984; Garver *et al*.,

Table 5. Elemental ratios of the analyzed samples from AAS analysis.

Well	Depth (ft)	V/Ni	Co/Mo	Th/Sr	Zr/Sr	Rb	Sr/Ba
DS	12300	2.7333	1.60E-07	0	0	19.21	2.28856
DS	12630	—	4.11E-05	0	34.34091	21.24	0.72
DS	12960	76.3636	1.80E-07	0	23.9601	25.07	1.0025
DS	13290	2.2651	1.80E-07	0	0.08611	40.31	16.3636
DS	13500	—	1.42E-04	0	27.8125	35.09	0.91624
ML 1	7840	0.6133	6.70E-07	0	0	25.2	1.09091
ML 1	8060	—	5.00E-05	0	0	25.23	1.34375
ML 1	8220	0.765	6.67E-06	0	0	26.08	2.6875
ML 1	8440	—	1.36E-03	0	19.2	40.23	1.51515
ML 1	8660	0.7017	1.80E-04	0	0	32.02	1.41667
ML 2	13240	—	1.14E-04	0	30.13245	22.1	0.70233
ML 2	13510	—	1.67E-04	0	25.5556	24.33	0.77436
ML 2	13720	23.72	4.17E-06	0	19.1667	27.05	2.90323
ML 2	14140	—	7.00E-05	0	29.3548	40.35	0.70588
ML 2	14530	—	1.89E-04	0.00645	21.6667	30.08	0.144

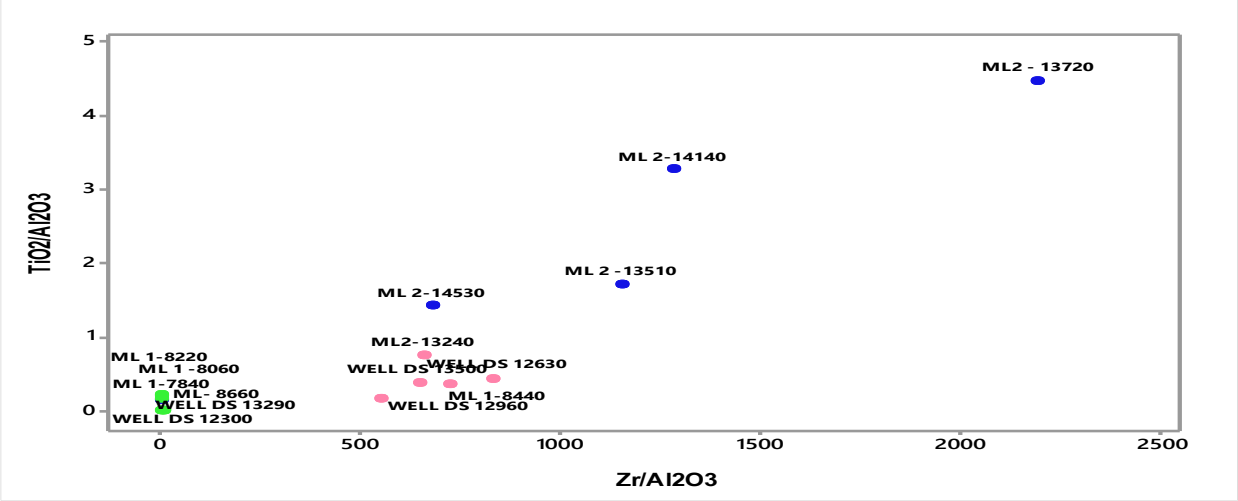

Figure 16. Showing plot of TiO_2/Al_2O_3 vs. Zr/ Al_2O_3 diagram for the study wells.

1994, 1996). High Cr and Ni concentrations in shales reflect their incorporation into clay particles during weathering of chromite and other Cr- and Ti-bearing minerals in the mafic/ultramafic rocks (Garver *et al*., 1996). Weak correlation between Cr and Ni indicates that the rocks containing these elements are of felsic composition (Garver *et al*., 1996). The Cr content of the rocks ranges from 200.00 to 4100.00 ppm (averaging 27.53 ppm) and the Ni content, from 0,001 to 3600 ppm (averaging 24.00 ppm). The plot of Cr and Ni contents of the study section reveals lower enrichment of Ni with respect to Cr (Figure 16). The Cr vs Ni plot shows a weak but positive correlation. These indicate that the sediments were derived from granitic or felsic terrain, following Garver *et al*. (1996). The study wells were therefore sourced from granitic/intermediate rocks, in a wet, humid climate. The most probable direction of granitic/intermediate provenance is from east of the basin due to its composition of the rocks and proximity of the study area (Figure 17).

Change in paleoweathering

The degree of compositional maturity of shales is estimated using the weathering index, as described by Kronberg and Nesbitt (1981). In the erosion index plot of $(Na_2O+K_2O)/(Al_2O_3+Na_2O+K_2O)$ vs $(SiO_2+Na_2O+K_2O)/(SiO_2+Al_2O_3+Na_2O+K_2O)$, it is shown that the rock

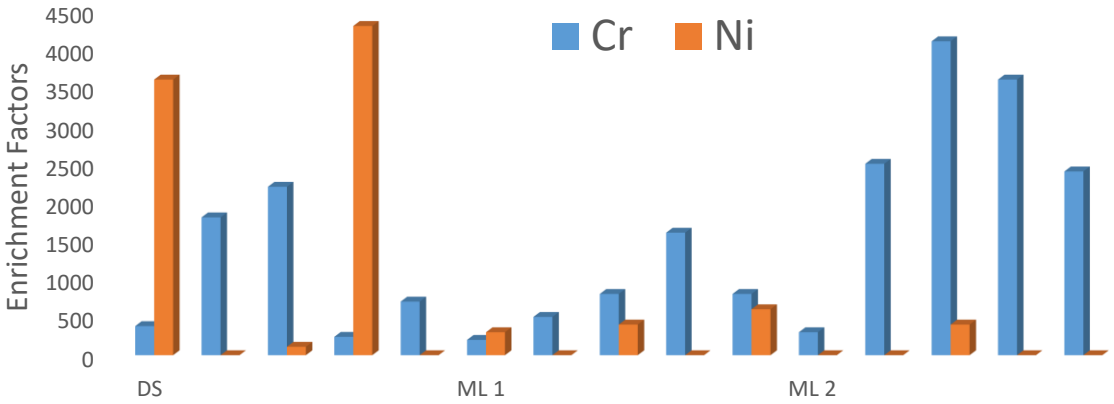

Figure 17. Showing Cr and Ni enrichment factors showing Cr enrichment relative to Ni the study well.

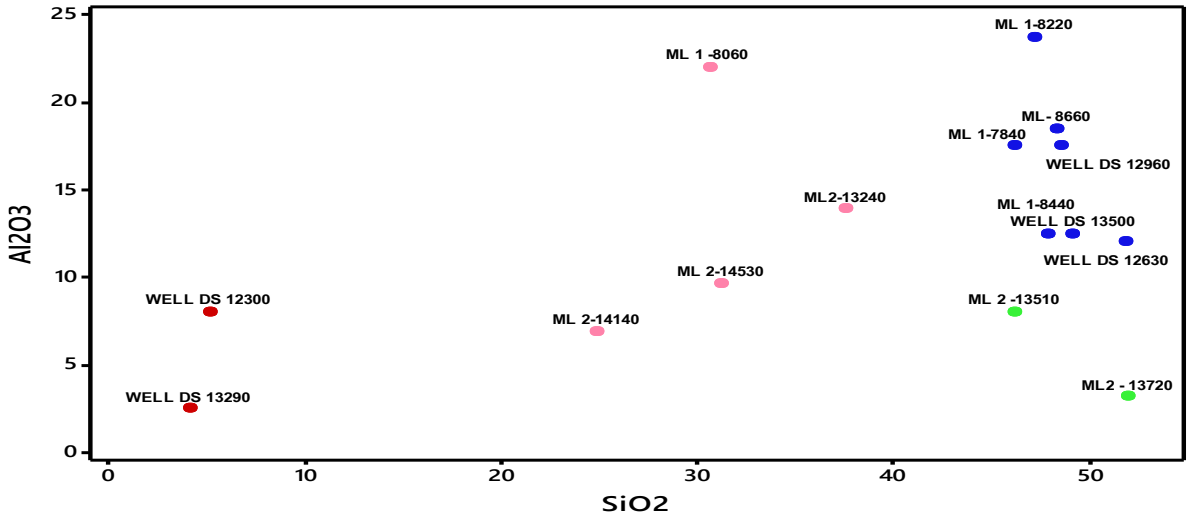

Figure 18. Showing Plot of Weathering Index of the study wells showing degree of weathering of the source area of the rocks.

samples from the ML 1 and ML 2 wells areas are plotted in the Kaolinite Field, while the rock samples from the DS well are plotted within the K-feldspar Field (Figure 18). The K_2O/Al_2O_3 ratio of rocks can be used as an indicator of the original composition of ancient rocks. Cox *et al*. (1995) showed that K_2O/Al_2O_3 ratios for clay minerals and feldspars differ. For clay minerals, the ratio is 0.00 to 1.00, and for feldspars, 0.30 to 0.90. The wells under study have K_2O/Al_2O_3 ratios from 0.016 to 0.068 (averaging 0.03). These indicate the presence of clay minerals and feldspar within the lower limit of their ranges (Kaolinite and Orthoclase). This agrees with the erosion index plot as the ditch cutting samples are plotted within the Kaolinite and K-feldspar (Orthoclase) domains. Figure 18, a plot of TiO_2 and Zr for discriminating source rock lithology for the three wells 12,300-13,500 ft, 7,840-8,660 ft and 13,240 ft sandstones, indicate that the sandstones of the 7,840-8,660 ft are sourced from intermediate rocks which are normally found on Continental Crust or Continental Arcs (Selegha *et al*., 2020) (Figure 18). Plot of TiO_2 and Zr for the complete well sections shows that all the sediments that comprise the formations transverse by the wellbore are derived from intermediate rock, which potentially are sourced from Continental Crust (Craigie, 2018; Ramkumar, 2015). The SiO_2 and Al_2O_3 have been used to understand the relationship between sandstone and clay in sediments. In this study, Figure 18, a binary plot of SiO_2 and Al_2O_3 shows a linear relationship for both SiO_2 and Al_2O_3, for all the samples from the wellbore. However, the majority of the samples (A) occur between 30 to 60% of silica with relatively high values of Al_2O_3. This observation is indicative of sediments that are derived from interme-

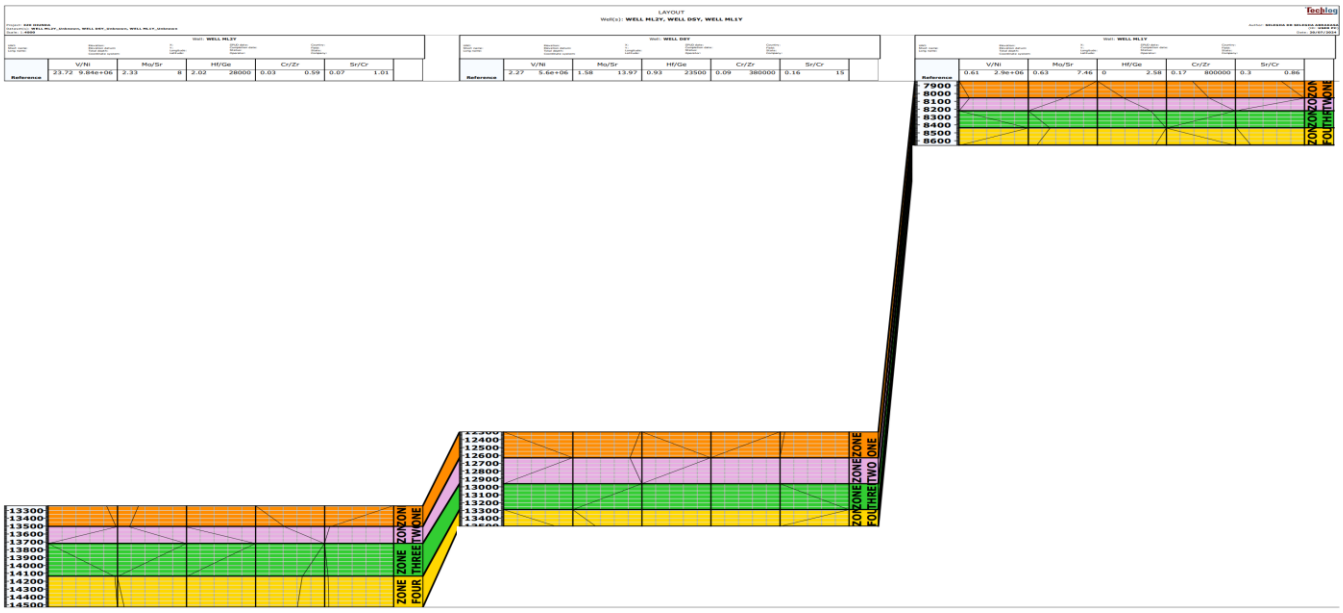

Figure 19. Showing Chemostratigraphic correlation for DS, ML 1 and ML 2 wells, with the plotted geochemical profiles for V/Ni, Mo/Sr, Hf/Ge, Cr/Zr and Sr/Cr. The transversal dotted lines plotted on each track shows the threshold values used to characterize each geochemical zone.

diate rock, which are sourced mostly from Continental Arcs. Some samples (B) bear lower silica values and consequently, lower values of Al_2O_3; these represent mafic sources derived from Oceanic Crust (Craigie, 2018; Ramkumar, 2015). It is inferred that there was a change in sediment source during the deposition of the sedimentary sequence in ML 1 and ML 2 wells. Furthermore, from the discriminant function diagram, it is inferred that the sandstones in the DS well are from a felsic igneous source, while those of ML 1 well are from a mafic igneous source. Inference from the provenance studies depicts that during the deposition of the claystones, siltstones and sandstones in study wells, sediment supply changed from an intermediate igneous source to a felsic igneous source because all the claystones in the wells plotted in the region of an intermediate igneous source on the discriminant diagram and the claystones were deposited first followed by the siltstones and the sandstones.

Chemostratigraphic correlation of the study wells

A correlation for the three wells was achieved based on inorganic geochemistry; this correlation was independent of the geology and mineralogy (Figure 19). Therefore, there was a need to understand the likely mineralogical control on these geochemical key elements that were used for the correlation. By this, additional geological information was derived from the correlation that was based on inorganic geochemistry. Figure 19 shows an overview of the chemostratigraphic correlation, including the geochemical profile of selected ratios between the studied wells. The correlation scheme preparation starts by plotting all the elemental data in a profile. Binary and ternary diagrams of the elements and ratios that show variation along the depth profile help to evaluate the sample distribution and to preliminary asses the zonation strength of different geochemical proxies. Subsequently, follows the identification of the key elements and elemental ratios that distinguish between the MZ 1, MZ 2, MZ 3 and MZ 4 zones with a high level of zonation confidence. The proposed correlation scheme for the three wells is strong, with over 85% zonation confidence. All four geochemical zones are recognised in DS, ML 1 and ML 2 wells, pointing to a correlation scheme that is accurate for the study wells. The shading between the element and elemental ratios curves enhances the visualisation of the correlation log between the three offset wells. Changes in shading colour or area usually indicate a different zone (Figure 19).

Conclusions

The plot of the geochemical signatures of major oxides concentrations suggests that there are at least four chemostratigraphic boundaries in the DS, ML 1 and ML 2 wells. The V/Ni ratio indicates redox environment. The ratio indicates that the sandstone series of DS at depth 12,300 to 13,500 ft, ML 1 well at depth 7,840 to 8,660 ft and ML 2 at depth 13,240 to 14,530 ft were deposited in

anoxic anoxic-rich nearshore environment to a shallow inner-middle marine environment. While sediments of 8,440 ft to 8,660 ft, 12,630 ft to 13,290 ft and from 13,240ft to 13,720 ft bear very high values, indicating more marine environments. The Fe_2O_3+MgO parameter shows that the sandstones of ML 1 at depth 14,140 to 14,530 ft have very low Fe_2O_3+MgO values, implying their source to be from Continental Crust, while the lower series of DS at depth 12,630 to 13,290 ft have very high values, indicating their source to be Oceanic Crust. The Al/bases ratio in DS well clearly discriminates between 12,800 to 13,000 ft sandstones, which have a low Al/bases ratio, implying pervasive weathering, which corresponds to a humid and wet climate. The TiO_2–Zr binary diagram shows that the majority of the samples were derived from a source with lithology which corresponds to Continental Crust and Continental Arcs; the chemostratigraphic sand unit correlation deviates from the lithostratigraphic sand correlation to an extent that may impact gas production. The variation between chemo - and biostratigraphic correlation is potentially vitally important for building reservoir models in the wells of study. This inference was supported by V/Sc, Ni/V and V/(V+Ni) ratios, all pointing to extensive dysoxic–anoxic conditions. Conversely, the interpretation from paleoredox proxies, V, U/Th, Th/U, V/Cr, indicates dominance of oxic conditions, and this information contradicts the physical observations of most of the shaly strata, which lack bioturbations.

CONFLICT OF INTEREST

The authors declare that they have no conflict of interest.

REFERENCES

Abrakasa, S., Okechukwu, N., & Edikan, S. (2020). General Chemostratigraphy of the formations in Well M, Offshore Senegal. *International Journal of Scientific Research and Engineering Development*, *3*(6), 2581-7175.

Akaegbobi, I. M., & Ogungbesan, G. O. (2016). Geochemistry of the Paleocene limestones of Ewekoro Formation, eastern Dahomey Basin, southwestern Nigeria: implication on provenance and depositional conditions. *Ife Journal of Science*, *18*(3), 669-684.

Algeo, T. J., & Maynard, J. B. (2004). Trace-element behavior and redox facies in core shales of Upper Pennsylvanian Kansas-type cyclothems. *Chemical Geology*, *206*(3-4), 289-318.

Aplin, A. C. (1993). The composition of authigenic clay minerals in recent sediments: Links to the supply of unstable reactants. In: Manning, D. A. C., Hall, P. L., & Hughes, C. R. (eds.). *Geochemistry of clay-pore fluid interactions*. Chapman and Hall. Pp. 81-106.

Armstrong-Altrin, J. S., Lee, Y. I., Verma, S. P., & Ramasamy, S. (2004). Geochemistry of sandstones from the Upper Miocene Kudankulam Formation, southern India: implications for provenance, weathering, and tectonic setting. *Journal of sedimentary Research*, *74*(2), 285-297.

Avbovbo, A. A. (1978). Tertiary lithostratigraphy of Niger Delta. *Amerian Association of Petroleum Geologists Bulletin*, *62*(2), 295-300.

Bhatia, M. R. (1983). Plate tectonics and geochemical composition of sandstones. *The Journal of geology*, *91*(6), 611-627.

Breit, G. N., & Wanty, R. B. (1991). Vanadium accumulation in carbonaceous rocks: a review of geochemical controls during deposition and diagenesis. *Chemical Geology*, *91*(2), 83-97.

Brumsack, H. J. (2006). The trace metal content of recent organic carbon-rich sediments: Implications for Cretaceous black shale formation. *Palaeogeography, Palaeoclimatology, Palaeoecology*, *232*(2-4), 344-361.

Calvert, S. E., & Pedersen, T. F. (2007). Chapter fourteen elemental proxies for palaeoclimatic and palaeoceanographic variability in marine sediments: interpretation and application. *Developments in Marine Geology*, *1*, 567-644.

Chamley, H. (1989). Clay Sedimentology. Springer Verlag, Berlin. p.623.

Childress, M., & Grammer, G. M. (2015). High resolution sequence stratigraphic architecture of a mid-continent Mississippian outcrop in southwest Missouri. Shale Shaker. Pp. 206-234.

Churchman, G. J. (2000). The alteration and formation of soil minerals by weathering. In: Summer, M.E. (ed.), *Handbook of soil science*. CRC Press, New York. 1, F3-27.

Cox, R., Lowe, D. R., & Cullers, R. L. (1995). The influence of sediment recycling and basement composition on evolution of mudrock chemistry in the southwestern United States. *Geochimica et Cosmochimica Acta*, *59*(14), 2919-2940.

Craigie, W. N. (2018). Principles of elemental chemostratigraphy. Cham: Springer.

Doust, H., & Omatsola, E. (1990). Niger Delta. In: Edwards, J. D., & Santogrossi, P. A. (eds.), Divergent/passive margin basins, *American Association of Petroleum Geologists Memoir, 48*, 201-239

Ehinola, O. A., Ejeh, O. I., & Oderinde, O. J. (2016). Geochemical characterization of the Paleocene Ewekoro limestone formation, SW Nigeria: implications for provenance, diagenesis and depositional environment. *Geomaterials*, *6*(3), 61-77.

Ejedawe, J. E., Coker, S. J. L., Lambert-Aikhionbare, D. O., Alofe, K. B., & Adoh, F. O. (1984). Evolution of oil-generative window and oil and gas occurrence in Tertiary Niger Delta Basin. *American Association of Petroleum Geologists Bulletin*, *68*(11), 1744-1751.

Evamy, B. D., Haremboure, J., Kamerling, P., Knapp, W. A. Molloy, F. A. and Rowlands, P.H. (1978). Hydrocarbon habitat of Tertiary Niger Delta. *American Association of Petroleum Geologists Bulletin 62*, 1-39.

Frankl, E. J., & Cordry, E. A. (1967). The Niger Delta oil province: Recent development onshore and offshore. *In Seventh World Petroleum Congress Proceedings, Mexico*, 2, 195-209.

Fu, X., Wang, J., Chen, W., Feng, X., Wang, D., Song, C., & Zeng, S. (2016). Elemental geochemistry of the early Jurassic black shales in the Qiangtang Basin, eastern Tethys: constraints for palaeoenvironment conditions. *Geological Journal*, *51*(3), 443-454.

Garver, J. I., Royce, P. R., & Scott, T. J. (1994). The presence of ophiolites in tectonic highlands as determined by chromium and nickel anomalies in synorogenic shale: Two examples from

North America. *Russian Geology and Geophysics*, *35*(2), 1-8.
Garver, J. I., Royce, P. R., & Smick, T. A. (1996). Chromium and nickel in shale of the Taconic foreland; a case study for the provenance of fine-grained sediments with an ultramafic source. *Journal of Sedimentary Research*, *66*, 100-106.
Ghandour, I. M., Masuda, H., & Maejima, W. (2003). Mineralogical and chemical characteristics of Bajocian-Bathonian shales, G. Al-Maghara, North Sinai, Egypt: climatic and environmental significance. Geochemical Journal, 37(1), 87-108.
Haack, R. C., Sunderaman, P., Diedjomahor, J. O., Xiao, H., Gant, N. J., May, E. D., & Kelsch, K., 2000. Niger Delta Petroleum System, Nigeria. In: Mello, M. R. & Kat, B. J. (eds). *Petroleum Systems of South Atlantic Margins*. Tulsa: America Association of Petroleum Geologist. Pp. 213-231.
Hallam, A., Grose, J. A., & Ruffell, A. H. (1991). Palaeoclimatic significance of changes in clay mineralogy across the Jurassic-Cretaceous boundary in England and France. *Palaeogeography, Palaeoclimatology, Palaeoecology, 81*(3-4), 173-187.
Hatch, J. R., & Leventhal, J. S. (1992). Relationship between inferred redox potential of the depositional environment and geochemistry of the Upper Pennsylvanian (Missourian) Stark Shale Member of the Dennis Limestone, Wabaunsee County, Kansas, USA. *Chemical Geology*, *99*(1-3), 65-82.
Hiscott, R. N. (1984). Ophiolitic source rocks for Taconic-age flysch: trace-element evidence. *Geological Society of America Bulletin*, *95*(11), 1261-1267.
Hou, H., Shao, L., Li, Y., Liu, L., Liang, G., Zhang, W., Wang, X., & Wang, W. (2022). Effect of paleoclimate and paleoenvironment on organic matter accumulation in lacustrine shale: Constraints from lithofacies and element geochemistry in the northern Qaidam Basin, NW China. *Journal of Petroleum Science and Engineering*, *208*, 109350.
Islam, M. R., Stuart, R., Risto, A., & Vesa, P. (2002). Mineralogical changes during intense chemical weathering of sedimentary rocks in Bangladesh. *Journal of Asian Earth Sciences*, *20*(8), 889-901.
Jia, J., Bechtel, A., Liu, Z., Strobl, S. A., Sun, P., & Sachsenhofer, R. F. (2013). Oil shale formation in the Upper Cretaceous Nenjiang Formation of the Songliao Basin (NE China): Implications from organic and inorganic geochemical analyses. *International Journal of Coal Geology*, *113*, 11-26.
Jones, B., & Manning, D. A. (1994). Comparison of geochemical indices used for the interpretation of palaeoredox conditions in ancient mudstones. *Chemical Geology*, *111*(1-4), 111-129.
Kronberg, B. I., & Nesbitt, H. W. (1981). Quantification of weathering, soil geochemistry and soil fertility. *Journal of Soil Science*, *32*(3), 453-459.
Lane, H. R., & De Keyser, T. L. (1980). Paleogeography of the late Early Mississippian (Tournaisian 3) in the central and southwestern United States. Paleozoic Paleogeography of West-Central United States: Rocky Mountain Paleogeography Symposium 1, pp. 149-162.
Letnikova, E. F., & Geletii, N. K. (2005). Vendian-Cambrian carbonate sequences in sedimentary cover of the Tuva-Mongol microcontinent. *Lithology and Mineral Resources*, *40*(2), 167-177.
Lewan, M. D. (1984). Factors controlling the proportionality of vanadium to nickel in crude oils. *Geochimica et Cosmochimica Acta*, *48*(11), 2231-2238.
Li, L., Liu, Z., George, S. C., Sun, P., Xu, Y., Meng, Q., ... & Wang, J. (2019a). Lake evolution and its influence on the formation of oil shales in the Middle Jurassic Shimengou Formation in the Tuanyushan area, Qaidam Basin, NW China. *Geochemistry, 79*(1), 162-177.
Li, M., Shao, L. Y., Liu, L., Lu, J., Spiro, B., Wen, H. J., & Li, Y. H. (2016). Lacustrine basin evolution and coal accumulation of the Middle Jurassic in the Saishiteng coalfield, northern Qaidam Basin, China. *Journal of Palaeogeography*, *5*(3), 205-220.
Li, Y., Sun, P., Liu, Z., Xu, Y., Liu, R., & Ma, L. (2021). Factors controlling the distribution of oil shale layers in the Eocene Fushun Basin, NE China. *Marine and Petroleum Geology*, *134*, 105350.
Li, Y., Wang, Z., Gan, Q., Niu, X., & Xu, W. (2019b). Paleoenvironmental conditions and organic matter accumulation in Upper Paleozoic organic-rich rocks in the east margin of the Ordos Basin, China. *Fuel*, *252*, 172-187.
Madukwe, H. Y., & Bassey, C. E. (2015). Geochemistry of the Ogwashi-Asaba Formation, Anambra Basin, Nigeria: Implications for provenance, tectonic setting, source area weathering, classification and maturity. International Journal of Science and Technology, 4(7), 312-327.
Maslov, A. V., Krupenin, M. T., & Gareev, E. Z. (2003). Lithological, lithochemical and geochemical indicators of paleoclimate: Evidence from Riphean of the Southern Urals. *Lithology and Mineral Resources*, *38* (5), 427-446,
Mazzullo, S. J., Boardman, D. R., Wilhite, B. W., Godwin, C., & Morris, B. T. (2013). Revisions of outcrop lithostratigraphic nomenclature in the Lower to Middle Mississippian Subsystem (Kinderhookian to Basal Meramecian series) along the shelf-edge in southwest Missouri, northwest Arkansas, and northeast Oklahoma. *The Shale Shaker*, 63(6), 414-454.
McLennan, S. M. (2001). Relationships between the trace element composition of sedimentary rocks and upper continental crust. *Geochemistry, Geophysics, Geosystems, 2*(4), 24.
Meng, Q., Liu, Z., Bruch, A. A., Liu, R., & Hu, F. (2012). Palaeoclimatic evolution during Eocene and its influence on oil shale mineralisation, Fushun basin, China. *Journal of Asian Earth Sciences*, *45*, 95-105.
Mohriak, W., & Talwani, M. (Eds.) (2000). *Atlantic rifts and continental margins*. American Geophysical Union, Washington, DC. 353p.
Munnecke, A., Calner, M., Harper, D. A., & Servais, T. (2010). Ordovician and Silurian sea–water chemistry, sea level, and climate: a synopsis. *Palaeogeography, Palaeoclimatology, Palaeoecology*, *296*(3-4), 389-413.
Murphy, M. A., & Salvador, A. (1999). International stratigraphic guide—an abridged version. *Episodes Journal of International Geoscience*, *22*(4), 255-271.
Nairn A. E. M., & Stahli, F. G. (1974). The occean basin and margins. The North Atlantic. Plenum Press, New York. Volume 2, 613p.
Nemcok, M. (2016). *Rifts and passive margins. Structural Architecture, thermal Regimes and petroleum systems*. Cambridge University Press. 620p.
Odoma, A. N., Obaje, N. G., Omada, J. I., Idakwo, S. O., & Erbacher, J. (2013). Paleoclimate reconstruction during Mamu Formation (Cretaceous) based on clay mineral distributions. *IOSR Journal of Applied Geology and Geophysics*, *1*(5), 40-46.
Osokin, P. V. (1999). Central Asian phosphorite-bearing province (stratigraphy and phosphorite potential). *Doctoral (Geology*

Mineral) Dissertation as a Scientific Report [in Russian]. GI SO RAN, Ulan-Ude.
Pettijohn, F. J., Potter, P. R. & Siever, R., (1987). Sand and sandstones. Springer, New York, 2nd Edition. 553p.
Ramkumar, M. U. (2015). Chemostratigraphy: Concepts, Techniques, Applications. Elsevier Radarweg, Amsterdam. 527p.
Ramkumar, M., Nagarajan, R., & Santosh, M. (2021). Advances in sediment geochemistry and chemostratigraphy for reservoir characterization. *Energy Geoscience*, *2*(4), 308-326.
Rangel, A., Parra, P., & Niño, C. (2000). The La Luna formation: chemostratigraphy and organic facies in the Middle Magdalena Basin. *Organic Geochemistry*, *31*(12), 1267-1284.
Ratcliffe, K. T., Morton, A. C., Ritcey, D. H., & Evenchick, C. A. (2007). Whole-rock geochemistry and heavy mineral analysis as petroleum exploration tools in the Bowser and Sustut basins, British Columbia, Canada. *Bulletin of Canadian Petroleum Geology*, *55*(4), 320-336.
Reijers, T. J. A. (2011). Stratigraphy and sedimentology of the Niger Delta. *Geologos*, 2011, 17 (3): 133-162.
Rimmer, S. M. (2004). Geochemical paleoredox indicators in Devonian–Mississippian black shales, central Appalachian Basin (USA). *Chemical Geology*, *206*(3-4), 373-391.
Roser, B. P., & Korsch, R. J. (1986). Determination of tectonic setting of sandstone-mudstone suites using SiO2 content and K2O/Na2O ratio. *The Journal of Geology*, *94*(5), 635-650.
Ross, D. J., & Bustin, R. M. (2006). Sediment geochemistry of the lower Jurassic Gordondale member, northeastern British Columbia. *Bulletin of Canadian Petroleum Geology*, *54*(4), 337-365.
Sarı, A., & Koca, D. (2012). An approach to provenance, tectonic and redox conditions of Jurassic-Cretaceous Akkuyu Formation, Central Taurids, Turkey. *Bulletin of the Mineral Research and Exploration*, *144*(144), 51-74.
Shen, Y., Qin, Y., Wang, G. G., Guo, Y., Shen, J., Gu, J., Xiao, Q., Zhang, T., Zhang, C., & Tong, G. (2017). Sedimentary control on the formation of a multi-superimposed gas system in the development of key layers in the sequence framework. *Marine and Petroleum Geology*, *88*, 268-281.
Short, K. C., & Stäuble, A. J. (1967). Outline of geology of Niger Delta. *American Association of Petroleum Geologists Bulletin*, *51*(5), 761-779.
Song, Y., Cao, Q., Li, S., Hu, S., Zhu, K., Ye, X., & Wan, L. (2021). Salinized lacustrine organic-rich shale influenced by marine incursions: Algal-microbial community, paleoenvironment and shale oil potential in the Paleogene Biyang Depression, East China. *Palaeogeography, Palaeoclimatology, Palaeoecology*, *580*, 110621.
Song, Y., Liu, Z., Sun, P., Meng, Q., & Liu, R. (2017). A comparative geochemistry study of several oil shale-bearing intervals in the Paleogene Huadian Formation, Huadian Basin, Northeast China. *Journal of Earth Science*, *28*(4), 645-655.
Sun, P., Sachsenhofer, R. F., Liu, Z., Strobl, S. A., Meng, Q., Liu, R., & Zhen, Z. (2013). Organic matter accumulation in the oil shale-and coal-bearing Huadian Basin (Eocene; NE China). *International Journal of Coal Geology*, 105, 1-15.
Sweere, T., van den Boorn, S., Dickson, A. J., & Reichart, G. J. (2016). Definition of new trace-metal proxies for the controls on organic matter enrichment in marine sediments based on Mn, Co, Mo and Cd concentrations. *Chemical Geology*, *441*, 235-245.
Tappan, H. (1968). Primary production, isotopes, extinctions and the atmosphere. *Palaeogeography, Palaeoclimatology, Palaeoecology*, *4*(3), 187-210.
Taylor, S. R., & McLennan, S. M. (1985). The continental crust, its composition and evaluation. Oxford: Blackwell.
Tribovillard, N., Algeo, T. J., Lyons, T., & Riboulleau, A. (2006). Trace metals as paleoredox and paleoproductivity proxies: An update. *Chemical geology*, *232*(1-2), 12-32.
Turner, B. W., Tréanton, J. A., & Slatt, R. M. (2016). The use of chemostratigraphy to refine ambiguous sequence stratigraphic correlations in marine mudrocks. An example from the Woodford Shale, Oklahoma, USA. *Journal of the Geological Society*, *173*(5), 854-868.
Vishnevskaya, I. A., & Letnikova, E. F. (2013). Chemostratigraphy of the Vendian–Cambrian carbonate sedimentary cover of the Tuva-Mongolian microcontinent. *Russian Geology and Geophysics*, *54*(6), 567-586.
Von Eynatten, H., & Gaupp, R. (1999). Provenance of Cretaceous synorogenic sandstones in the Eastern Alps: constraints from framework petrography, heavy mineral analysis and mineral chemistry. *Sedimentary Geology*, *124*(1-4), 81-111.
Von Rad, U., Hinz, K., Sarnthein M., & Seibold, E. (1982). Geology of the Northwest African Continental Margin. Springer, Berlin, 709p
Wang, Z., Wang, J., Fu, X., Zhan, W., Armstrong-Altrin, J. S., Yu, F., Feng, X., Song, C., & Zeng, S. (2018). Geochemistry of the Upper Triassic black mudstones in the Qiangtang Basin, Tibet: Implications for paleoenvironment, provenance, and tectonic setting. *Journal of Asian Earth Sciences*, *160*, 118-135.
Weber, K. J., & E.M. Daukoru, 1975. Petroleum geological aspects of the Niger Delta. *Nigeria Journal of Mining and Geology,* 12(1/2), 9-22.
Wei, W., & Algeo, T. J. (2020). Secular variation in the elemental composition of marine shales since 840 Ma: Tectonic and seawater influences. *Geochimica et Cosmochimica Acta*, *287*, 367-390.
Wu, Y., Liu, C., Liu, Y., Gong, H., Awan, R. S., Li, G., & Zang, Q. (2022). Geochemical characteristics and the organic matter enrichment of the Upper Ordovician Tanjianshan Group, Qaidam Basin, China. *Journal of Petroleum Science and Engineering*, *208*, 109383.
Xi, D., Wan, X., Jansa, L., & Zhang, Y. (2011). Late Cretaceous paleoenvironment and lake level fluctuation in the Songliao Basin, northeastern China. *Island Arc*, *20*(1), 6-22.
Xin, B., Hao, F., Han, W., Xu, Q., Zhang, B., & Tian, J. (2021). Paleoenvironment evolution of the lacustrine organic-rich shales in the second member of Kongdian Formation of Cangdong Sag, Bohai Bay Basin, China: Implications for organic matter accumulation. *Marine and Petroleum Geology*, *133*, 105244.
Zeng, S., Wang, J., Fu, X., Chen, W., Feng, X., Wang, D., Song, C., & Wang, Z. (2015). Geochemical characteristics, redox conditions, and organic matter accumulation of marine oil shale from the Changliang Mountain area, northern Tibet, China. *Marine and Petroleum Geology*, *64*, 203-221.
Zhang, L., Dong, D., Qiu, Z., Wu, C., Zhang, Q., Wang, Y., Liu, D., Deng, Z., Zhou, S., & Pan, S. (2021). Sedimentology and geochemistry of Carboniferous-Permian marine-continental transitional shales in the eastern Ordos Basin, North China. *Palaeogeography, Palaeoclimatology, Palaeoecology, 571*, 110389.
Zhang, X., Gao, Z., Fan, T., Xue, J., Li, W., Zhang, H., & Cao, F.

(2020). Element geochemical characteristics, provenance attributes, and paleosedimentary environment of the Paleogene strata in the Lenghu area, northwestern Qaidam Basin. *Journal of Petroleum Science and Engineering*, *195*, 107750.

Zhu, B., Yang, T., Wang, J., Chen, X., Pan, W., & Chen, Y. (2022). Multiple controls on the paleoenvironment of the early Cambrian black shale-chert in the northwest Tarim Basin, NW China: Trace element, iron speciation and Mo isotopic evidence. *Marine and Petroleum Geology*, *136*, 105434.